KERNFORSCHUNGSZENTRUM

KARLSRUHE

November 1972 KFK 1627

Institut für Neutronenphysik und Reaktortechnik
Projekt Schneller Brüter

KINTIC-1: A program for the calculation of two-dimensional reactor dynamics of fast reactors with the quasistatic method

L. Mayer and H. Bachmann

GESELLSCHAFT FÜR KERNFORSCHUNG M. B. H.

KARLSRUHE

GESELLSCHAFT FÜR KERNFORSCHUNG M.B.H.
KARLSRUHE

KERNFORSCHUNGSZENTRUM KARLSRUHE

KFK 1627

Institut für Neutronenphysik und Reaktortechnik

Projekt Schneller Brüter

KINTIC-1: A program for the calculation of two-dimensional reactor dynamics of fast reactors with the quasistatic method

L. Mayer and H. Bachmann

Gesellschaft für Kernforschung mbH, Karlsruhe

Abstract

KINTIC-1 is the first version of a system of programs for treating all stages of a reactor excursion, starting with the initial perturbation and finishing, eventually, with core disassembly and a second excursion. Part 1 of this report gives a summary of the basic physical models underlying the program. It has been developed for two-dimensional geometry, using the quasistatic method for the neutron kinetics part. Currently, only external perturbations caused by some sort of material movement can be simulated. For the description of zone dependent thermodynamics in the core and blanket, a model with a single representative channel for each different reactor zone is employed. Feedback effects include space dependent density changes and expansion of reactor zones and cross section changes due to the Doppler effect. At present, coolant boiling, interaction of sodium and fuel etc. are not included.
The parameters of a problem (e.g. number of mesh points, of energy groups etc.) may be chosen freely within the limits of the available computer storage, since dynamic storage assignment has been used. Additionally, limits have been imposed on the number of energy groups (26), precursor groups (6), reactor material zones (1oo) and representative coolant channels (1o).

Part 1 of the report concludes with a short discussion of future extensions of KINTIC and with a presentation of some numerical calculations and comparisons. Part 2 contains input and control card lists, a small sample case, some information on program organization and flow charts. It is intended to enable a user to do his own calculations with KINTIC-1.

Kurzfassung

KINTIC-1 ist die erste Stufe eines Programmsystems zur Behandlung aller Stadien einer Reaktorexkursion, beginnend mit der einleitenden Störung bis zum eventuellen Zusammenschmelzen des Core und zur zweiten Exkursion. Im ersten Teil der vorliegenden Arbeit werden die physikalischen Modelle zusammengefaßt, die die Basis des Programms bilden. Es behandelt zweidimensionale Geometrie und benutzt die quasistatische Methode für den Neutronenkinetik-Teil. In der vorliegenden Version können nur Störungen simuliert werden, die durch eine Materialbewegung verursacht werden. Für die Beschreibung der zonenabhängigen Thermodynamik in Core und Blanket wird ein Einkanalmodell mit charakteristischen Kühlkanälen für verschiedene Reaktorzonen benutzt. Die Rückwirkungseffekte umfassen ortsabhängige Dichteänderungen und die

Ausdehnung von Reaktorzonen sowie Wirkungsquerschnittsänderungen aufgrund des Dopplereffekts. Zur Zeit können noch keine Effekte wie Kühlmittelsieden, Brennstoff-Natrium Reaktion usw. beschrieben werden.
Die Parameter eines Problems wie Zahl der Maschenpunkte, der Energiegruppen usw. können unter Rücksichtnahme auf den verfügbaren Kernspeicher frei gewählt werden, da eine dynamische Speicherplatzzuweisung realisiert wurde. Zusätzliche obere Grenzen sind: Bis zu 26 Energiegruppen, 6 Verläufergruppen, 1oo Materialzonen und 1o charakteristische Kühlkanäle.

Teil 1 der Arbeit wird abgeschlossen mit einer kurzen Diskussion der geplanten Codeerweiterungen und mit den Ergebnissen numerischer Rechnungen und Vergleiche. Teil 2 enthält Eingabe- und Kontrollkartenlisten, die Eingabe für eine kleine Proberechnung, einige Informationen über die Codeorganisation und Flußdiagramme. Er soll es dem Benutzer ermöglichen, selbständig Rechnungen mit KINTIC-1 durchzuführen.

Contents

Part 1: Theory and first results

I. Introduction

In recent years, the growing concern about reactor safety has given increasing importance to the development of methods for the calculation of the dynamic behaviour of power reactors. In principle, these methods should be able to account, in detail, for the various physical processes taking place during excursions: Space- and time-dependent neutron kinetics, thermodynamics and -hydraulics, coolant boiling, expulsion and reentry, fuel element failure and fuel-coolant interaction, core meltdown etc. Until recently, the available codes tended to stress only a few of these aspects: especially, since most codes consisted either of an elaborate thermodynamics and feedback model coupled to a simple point kinetics code or of a space dependent neutron kinetics module which had been outfitted with some very simple feedback equations. Though undeniably of great importance for the study of special effects of reactor dynamics, these codes were only of limited usefulness for the description of the whole spectrum of possible reactor perturbations and accidents. With the advent of bigger and faster computers, the development of comprehensive multi-dimensional codes became feasible and has been started by several groups /1-5/.

In Karlsruhe, a dual approach to the problem of multi-dimensional reactor dynamics for fast reactors has been taken. First, a two-dimensional code using discontinuous time-synthesis has been developed /1/. As this method is only an approximative one with no known convergence criteria, it was deemed necessary to have at least one other method for comparative studies. Because fully numerical codes in more than one dimension are still too time consuming on present day computers, the quasistatic approach to neutron kinetics /6/ has been chosen. This method, using only a few approximations, is quite fast due to the use of point kinetics for longer time intervals. On the other hand, if these intervals are decreased - and the computing time increased accordingly, - the method approaches a fully numerical calculation and thus is able to compute its own benchmark problems.

Zum Druck eingereicht am 11.12.1972

Using this method for the neutron kinetics part and relying on the feedback part of the synthesis code cited above, the two-dimensional dynamics code KINTIC-1 has been developed. In its present form, it will follow a reactor excursion only until coolant boiling or pin failure occurs.Though there are very interesting and important applications for such a code, e.g. evaluation of the importance of space-dependent kinetics, it should be viewed as the first stage in the development of a reactor excursion code which is able to handle the initial processes of an excursion as well as coolant boiling, core disassembly and second excursion. The addition of program parts for these processes are planned for the near future. Such extensions of the code are facilitated by its modular structure.In passing, it should be noted that the code is written in Fortran IV for an IBM-360.

The purpose of this report is to give a description of the physical models used in the quasistatic code in its present form. The actual code description giving the code organization, input, sample problem etc. forms the contents of the second part of the report. This first part should provide a basic understanding of the processes the code is able to describe, the models and approximations used and the different parameters involved. With the addition of further modules supplementary code descriptions will be issued.

The sequence of operations done by KINTIC-1 and its associated programs is as follows. First the nuclear data are evaluated using the appropriate modules from the Karlsruhe nuclear code system NUSYS /22/, which contains one special module for bringing the data into a form suitable for KINTIC-1. These data do not comprise the Doppler data, which must be evaluated in a separate run and fed into KINTIC-1 via punched cards produced by this run. One may then start KINTIC-1, which first calculates the steady state neutron, precursor and temperature distribution and may optionally perform a criticality search. It then proceeds with the transient calculations, alternately performing point kinetics calculations with estimates for the coefficients given by the quasistatic formalism, and recalculations of the temperature distribution. After longer time intervals, the so-called macro-intervals, the neutron distribution is recalculated using the quasistatic equations. New point kinetics coefficients result from this, which are compared to the estimates, and if necessary, the whole macro-interval is

recalculated. Then the calculation proceeds to the next macro-interval and continues in this way until the time interval, over which the excursion is to be followed has been computed. After the end of the transient calculation it is possible to start an evaluation run with the program DYNEVA, which works with a tape recording of the results created by KINTIC-1 to produce drawings of the results specified by the user.

The sequence of the next chapters more or less follows the sequence of operations performed by the code. The next two chapters deal with the treatment of nuclear data and with the stationary calculations preceding the dynamics. The fourth chapter gives an introduction to the quasistatic method used for the neutron kinetics. The following chapter is on the thermodynamics model and the treatment of feedback. The sixth chapter describes the approximation to the external perturbation causing the excursion. Some special features of the code are outlined in chapter VII. A special chapter has been reserved to a discussion of the methods of automatic time step length determination. In the ninth chapter, the alterations and extensions planned for the near future are listed. In the last chapter, results of calculations done with the code are discussed. These include comparisons with zero-dimensional calculations and with the fully numerical code MITKIN as well as calculations done for a superprompt critical experiment in SEFOR.

II. Treatment of nuclear data

The nuclear data used for dynamics calculations may be divided into three groups: Cross sections, excluding the temperature dependence; Doppler data, i.e. temperature derivatives of cross sections; data pertaining to the delayed neutrons. The present treatment of these data is outlined here. The concept used is under review and will probably be altered (see chapter IX).

For the preparation of the nuclear data, existing codes from the Karlsruhe NUSYS-system have been used to a large degree. The preparation of the nuclear data - in the NUSYS-routines - and their application - in KINTIC-1 - are completely seperated steps. This does not prevent the user from running the data compilation and a dynamics calculation in one job, but it enables him to prepare a data set for a special reactor and then use it for a number of different perturbation cases for the same reactor.

1. Cross sections. Considering the high amount of computer time necessary for a two-dimensional time dependent calculation, such computations for fast reactors have to be done at present with only a limited number of energy groups, usually 4 - 1o groups depending on the size of the entire problem and the importance of spectral shifts. The starting point for a few group cross section evaluation in Karlsruhe are the different 26-group cross section sets similar to the ABN-set /7/ and the ABN-set itself. Normally, these have to be condensed to a smaller number of groups using spectra from one- or two-dimensional diffusion calculations. Up to this point, the cross section evaluation resembles that for a normal diffusion calculation. However, in a dynamics calculation including feedback the different temperatures of fuel, coolant etc. resulting in different density changes for these materials must be taken into account. Therefore, the homogenized compositions in the reactor core, which are composed of a mixture of fuel, coolant etc. must be broken down into the contributions of these so-called macro-materials, namely fuel, can, coolant, structure material and, optionally, bounding. This is performed by a special NUSYS-program - 225o -, which in addition to this task adds the data for the perturbation causing the excursion and for the delayed neutrons to the data

block, brings it into a form suitable for KINTIC-1 and writes it into an external data set. KINTIC-1 may then proceed with the contents of this data set to do the dynamics calculations.

There is one special feature of the dynamics program which has a feedback on the cross section evaluation part, namely that no two reactor zones may have the same composition number. On the other hand, as reactor zones must be small enough to give a good representation of the spatial temperature dependence, there are normally a lot of zones with the same initial composition. Therefore, 225o contains an option which permits the user to duplicate each composition as often as necessary, ascribing new composition numbers to the duplicates. The same is true for the perturbations, which are defined as differences of compositions (see chapter VI). If a perturbation is the same in two or more reactor zones, it must nevertheless be defined for each zone seperately.

2. Doppler data. There are two possibilities for taking the Doppler effect into account. One is to calculate directly the temperature dependent cross sections of the heavy isotopes from the cross section sets available in Karlsruhe using the temperature dependent self-shielding factors from the data sets and the interpolation formulas provided by the NUSYS-modules. Second, one may use the Doppler program developed by R. Fröhlich and I. Siep /8,9/, which directly calculates the temperature derivatives of the macroscopic capture and fission cross sections using nuclear resonance data. This program is to be employed for the KINTIC-1 calculations, but in the current version, it is not yet integrated into the cross section evaluation part or KINTIC-1 itself. Rather, a control program, DOPKIN, has been written, which works within the framework of NUSYS and does the necessary organization, initiating repeated calls to the Doppler program for the calculation of the cross section temperature derivatives for the different compositions and temperatures, storing the results and, optionally, condensing them. The condensed derivatives themselves are not used, but a function approximating them

$$\frac{\partial \sigma}{\partial T} = a\left(\frac{T_o}{T}\right)^x \qquad (1)$$

is calculated with a least squares fit. The parameters a, x and T_o = 3oo ^oK are punched by DOPKIN for direct insertion into the input of KINTIC-1.

Equation (1) approximates the derivatives very well. The error is less than 1 % for temperatures up to 1500 ^{o}K and less than 2 - 4 % for higher temperatures.

3. Data of the delayed neutron groups. The parameters of the delayed neutron groups (delay fraction β_i, precursor decay constant λ_i and energy spectrum $\chi_i(E)$) are not included in the group cross section sets and must therefore be provided by the user. They form part of the input for the program 2250 mentioned above and are transferred to KINTIC-1 together with the cross sections. The values β_i and λ_i may depend on the fissionable isotope, $\chi_i(E)$ on the precursor group only.

III. Calculations for the stationary reactor

1. Geometrical representation of the reactor. KINTIC-1 is able to handle all two-dimensional geometries, i.e. r-z, x-y and r-θ, but for calculations including feedback r-z geometry must be chosen. As a result of feedback, reactor zones with identical material compositions initially get different cross sections and therefore must be distinguished by their composition numbers from the beginning (see chapter II); therefore, no two reactor zones may have the same composition number. For the representation of feedback, the core is subdivided radially into up to 1o segments. The temperatures are calculated for each of these segments using a representative cooling channel consisting of fuel, can, coolant and structure material. The axial temperature dependence is accounted for by subdividing the radial segments axially into up to 1o zones with representative temperatures in fuel, can etc. for each. The number of axial zones and their position must be the same for each radial segment. In addition to these feedback zones, the reactor may have non-feedback zones, e.g. reflector, central loop or control rod zones surrounding the feedback zones or inserted between them. For an example of one possible geometry see fig. 1. The reactor represented there has a two zone core, axial and radial blanket and reflector, central loop and partially inserted control rods. For the two-dimensional geometry, control rods in off-central positions have to be combined to control rod banks, with or without surrounding fuel elements; in the second case, the corresponding zones should form a feedback segment while in the first they are non-feedback zones.

The way in which the program distinguishes feedback and non-feedback zones as well as zones pertaining to different radial segments will be described in the second part of the report.

2. Stationary calculations. The first operation of KINTIC-1 is the determination of the static neutron distribution. Then, it must somehow achieve zero initial criticality so as to make sure that no fictitious transients are induced. There are different ways of doing this.

First, if k_{eff} is not too much different from 1, criticality may be achieved by simply dividing the number of neutrons per fission, ν by k_{eff}. This may

be the only action taken, but even if criticality is achieved by means of a criticality search to be described below, the small residual deviation of k_{eff} from 1 is always compensated in this way.

A second possibility consists in using the criticality search option provided by the diffusion program DIXY /1o/ which forms the basis of all flux distribution evaluations in KINTIC-1. There, criticality is achieved by enlarging or contracting axially or radially one of the reactor zones. In practice, this option allows the enlargement of a control rod zone or of a reflector until criticality is reached.

KINTIC-1 itself provides two criticality search options. In the first one, the reactor as a whole is expanded or contracted axially or radially to achieve criticality. The second one provides for a variation of the concentration of one macro-material in a limited number of zones. With this option, one may for example change the absorber concentration in a control rod until criticality is reached.

Another inconsistency remains in the case of a calculation including feedback. Here, the initial temperature distributions are, of course, space dependent, whereas the cross sections have been calculated by the NUSYS program usually for 9oo ^{o}K for the heavy isotopes and 3oo ^{o}K for all other isotopes. This discrepancy would not induce a big error into the dynamics calculations, because the feedback routines evaluate only the changes of the cross sections due to the changes of temperatures which are then added to their initial value. Nevertheless, there is an option providing the correct temperature dependent cross sections after the first criticality calculation and then doing a second diffusion calculation and temperature evaluation. An iteration of this process is not necessary as sufficiently accurate consistency of temperatures and cross sections is already achieved after the second diffusion calculation. There are two versions of this consistency calculation: The first one provides for consistent alterations of cross sections and densities; the second one only takes into account the cross section alterations due to Doppler effect, assuming that the densities have already been consistently determined in foregoing static calculations. The criticality iteration, if required, is started after this operation.

After consistency of cross sections and temperatures and exact criticality have been achieved, the program performs the remaining steady state calculations, i.e. evaluation of the adjoint flux and the space dependent precursor concentrations. It then proceeds with the dynamic calculations.

IV. The neutron kinetics part of KINTIC-1

As mentioned above, the quasistatic method is used for the neutron kinetics part of KINTIC-1. Here, a short derivation of the quasistatic equations will be given, its merits will be pointed out and the options available with KINTIC-1 will be listed. For further information on the quasistatic method, see /2, 6, 11/.

The derivation of the quasistatic equations given here follows closely those given in /6/ and /12/. The time dependent multigroup diffusion equations will be written in the form

$$\frac{1}{v_g}\frac{\partial \phi_g}{\partial t} = \nabla D_g \nabla \phi_g + \chi_g \sum_{g'} (1-\beta)\ \nu\Sigma^f_{g'}\ \phi_{g'} - \Sigma^{rem}_g\ \phi_g$$

$$+ \sum_{g'<g} \Sigma^s_{g'\to g}\ \phi_{g'} + \sum_i \chi^i_g\ \lambda_i\ C_i + Q_g \qquad (2)$$

with the left hand term signifying the change of neutron density in group g with time and the right hand terms giving the neutron gain through diffusion, prompt fission, removal, scattering, delayed neutrons and an external source. The usual notation has been employed. The external source has been included for generality, but the present code does not contain an option for initially subcritical reactors with a source. For the precursor densities

$$\frac{\partial C_i}{\partial t} = \sum_g \beta_i\ \nu\Sigma^f_g\ \phi_g - \lambda_i\ C_i \qquad (3)$$

The arguments have been dropped in equations (2) and (3), but of course all cross sections, fluxes, precursor densities as well as Q_g are space and time dependent; β, β_i and λ_i are material and therefore space dependent, χ_g and χ^i_g are constant.

The flux ϕ_g is now separated into

$$\phi_g(r,t) = A(t)\ \psi_g(r,t) \qquad (4)$$

with the assumption that the amplitude function, A is strongly time dependent and the shape function, ψ_g only weakly so.

The equation for A, the point kinetics equation, could be found by using only (2), (3) and the adjoint flux at time zero. The resulting expression for the reactivity ρ (eq. (32)) leads to numerical difficulties (differences of nearly equal numbers) which will be shortly discussed in chapter VII. Therefore, the adjoint equation at time zero is used as well in the derivation of the point kinetics equations. It is

$$0 = \nabla D_g^o \nabla \psi_g^* + (1-\beta)\, \nu\Sigma_g^{f,o} \sum_{g'} \chi_{g'}\, \psi_{g'}^* - \Sigma_g^{rem,o}\, \psi_g^*$$

$$+ \sum_{g'>g} \Sigma_{g\to g'}^{s,o}\, \psi_{g'}^* + \sum_i \beta_i\, \nu\Sigma_g^{f,o} \sum_{g'} \chi_{g'}^i\, \psi_{g'}^* \qquad (5)$$

By inserting (4) into (2) and (3), multiplying (2) with ψ_g^*, (3) for each energy group with $\psi_g^* \chi_g^i$ and (5) with $A\psi_g$ and utilizing the constraint for ψ

$$\int_{Vol} \sum_g \psi_g^* \frac{1}{v_g} \psi_g = \text{const} \qquad (6)$$

one derives the usual point kinetics equations:

$$\frac{dA}{dt} = \frac{\rho - \bar{\beta}}{l} A + \sum_i \lambda_i \bar{C}_i + \bar{Q} \qquad (7)$$

$$\frac{d\bar{C}_i}{dt} = \frac{\bar{\beta}_i}{l} A - \lambda_i \bar{C}_i \qquad (8)$$

The coefficients are given by the following equations:

$$\bar{C}_i = \frac{1}{I} \cdot \int_{Vol} \sum_g \psi_g^* \chi_g^i C^i \qquad (9)$$

$$\bar{Q} = \frac{1}{I} \int_{Vol} \sum_g \psi_g^* Q_g \qquad (1o)$$

$$\frac{\bar{\beta}_i}{l} = \frac{1}{I} \int_{Vol} \beta_i \sum_g \psi_g^* \chi_g^i \sum_{g'} \nu\Sigma_{g'}^f \psi_{g'} \tag{11}$$

$$\frac{\bar{\beta}}{l} = \sum_i \frac{\bar{\beta}_i}{l} \tag{12}$$

$$\begin{aligned}\frac{\rho}{l} = \frac{1}{I} \int_{Vol} \Bigg[& \sum_g \psi_g^* \nabla D_g \nabla\psi_g - \sum_g \psi_g \nabla D_g^o \nabla\psi_g^* + \\ & + (1-\beta) \sum_g \psi_g^* \chi_g \sum_{g'} \delta(\nu\Sigma_{g'}^f) \psi_{g'} + \\ & + \sum_i \beta_i \sum_g \psi_g^* \chi_g^i \sum_{g'} \delta(\nu\Sigma_{g'}^f) \psi_{g'} - \\ & - \sum_g \psi_g^* \delta(\Sigma_g^{rem}) \psi_g + \sum_g \psi_g^* \sum_{g'<g} \delta(\Sigma_{g'\to g}^s) \psi_{g'} \Bigg]\end{aligned} \tag{13}$$

$$I = \int_{Vol} \sum_g \psi_g^* \frac{1}{v_g} \psi_g \tag{14}$$

with

$$\delta(\Sigma) = \Sigma - \Sigma^o \tag{15}$$

being the deviation of the cross section from its initial value. Note that the coefficients are time dependent in two ways: Partly through the time dependent cross section which in turn result from the perturbation causing the excursion and the feedback, and partly through the time dependent shape function.

Up to this point, the treatment of the kinetics equations is common to a number of methods. For example, the point kinetics approximation employs only eq.s (7) and (8) using the initial cross sections and shape function or any other better suited shape function for the calculation of β and l and replacing the time dependence of ρ given by (13) by a suitable reactivity

ramp or other representation of the reactivity. Thus, the time dependent change of the shape function is not explicitly accounted for by the point kinetics method. The adiabatic approximation performs a recalculation of the shape function after longer time intervals employing the time independent diffusion equation. This introduces an error because the time derivatives and the time lag of precursor concentration and distribution are neglected and thus becomes inadequate for very fast transients. This difficulty is overcome by the quasistatic method, which, while recalculating the shape function only after long time intervals like the adiabatic method, employs basically the time dependent equation (2) with only a few approximations. Upon inserting (4) into (2), dividing by A(t) and rearranging the terms, one gets the quasistatic equation for the shape function

$$\frac{1}{v_g}\frac{\partial \psi_g}{\partial t} = \nabla D_g \nabla \psi_g + \chi_g \sum_{g'} (1-\beta)\, \nu\Sigma^f_{g'} \psi_{g'} - (\Sigma^{rem}_g + \frac{\dot{A}}{A})\psi_g + \sum_{g'<g} \Sigma^s_{g'\to g} \psi_{g'} + \frac{1}{A}\left(\sum_i \chi^i_g \lambda_i C_i + Q_g\right) \qquad (16)$$

There are two ways of dealing with the left hand term of equation (16):

1. Quasistatic:

$$\frac{1}{v_g}\frac{\partial \psi_g}{\partial t} = 0, \qquad (17)$$

i.e. it is assumed that due to the very small value of $1/v_g$ and the slow variation of ψ_g the term is very small compared to all other terms in (16).

2. Improved quasistatic:

$$\frac{1}{v_g}\frac{\partial \psi_g}{\partial t} = \frac{1}{v_g}\frac{\psi_g(t) - \psi_g(t-\Delta t)}{\Delta t}, \qquad (18)$$

with Δt signifying the time interval since the last shape function calculation. In this case, the time derivative is approximated by a backward difference.

One may now state the approximations inherent in the quasistatic method:

1. Recalculation of the shape function only after longer time intervals. In KINTIC-1, the shape function between two recalculations is approximated by a linear interpolation of the two functions. This error may be reduced by using smaller time intervals between the recalculations.
2. Approximation of the shape function time derivative by equation (17) or (18).

These are the only approximations of the quasistatic method. One may thus expect the method to produce very good results. The advantages and disadvantages of the method may be outlined as follows:

Advantages:

1. The very few approximations result in a method which stays very close to a fully numerical method and is much more exact than the adiabatic or point kinetics method. Especially, if small time intervals between the shape function calculations are used, the improved quasistatic method approaches a fully numerical implicit calculation.
2. For the usual large time intervals between shape function calculations the computation is much faster than a fully numerical one.
3. No guesses concerning the shape function must be employed contrary to all synthesis methods.
4. For the solution of the shape function equation, one of the usual multigroup diffusion codes with an option for source problems may be employed by using suitable redefinitions of the cross sections and the source. As may be seen from eq. (16), the fission cross section must be multiplied by $1 - \beta$, Σ_{rem} must be replaced by $\Sigma_{rem} + \dot{A}/A$ for the quasistatic and by $\Sigma_{rem} + \dot{A}/A + 1/(v_g \Delta t)$ for the improved quasistatic method. The source is given by the last line of eq. (16) for the quasistatic method, to which the term $\psi(t - \Delta t)/(v_g \Delta t)$ is added for the improved quasistatic method.

Disadvantages:

1. The method could require larger computing times than some direct numerical procedures, if many shape function recalculations are needed.

The program KINTIC-1 provides the following options in its kinetics part:

1. The quasistatic method. As yet, the improved quasistatic method has not been incorporated, but it is planned to do so.
2. A point kinetics option, using eq.s (11) - (13) with the steady state shape function for the determination of the coefficients.
3. The adiabatic method, i.e. shape function determination with the time independent diffusion equation.

Up to now $Q_g = 0$ in eq. (2), i.e. no external sources are allowed and consequently, no initially subcritical assemblies can be handled.

V. The thermodynamics and feedback model

The thermodynamics model is the same as in RADYVAR and therefore is described only briefly here. Further information may be gathered from /1/. It should be stressed that a new version of the thermodynamics module is being prepared and will be inserted in KINTIC upon its completion.

The geometrical representation of the reactor for feedback and thermodynamics has already been discussed in chapter III.1. As pointed out there, the reactor core and blanket are radially subdivided into up to 1o segments, to each of which is ascribed a representative coolant channel. The axial dependence of power and temperatures is described by subdividing the segment into up to 1o axial zones. With reflectors and non feedback zones, the reactor may then have a configuration like e.g. fig. 1. The representative coolant channel is described in cylindrical geometry with fuel, can, coolant and structure material. Representation of the radial temperature dependence within the fuel pellet is achieved by subdividing the fuel into up to 6 zones. The can is internally divided into two zones. Fig. 2 shows a sketch of the geometrical representation. Axial heat conduction is neglected.

A list of the equations for the temperature distribution will be given here with subscripts f, c, k and s denoting fuel, can, coolant and structure material, respectively. They are (/1/):

1. Fuel

$$\frac{\partial}{\partial r}\left(k_f \frac{\partial}{\partial r} T_f\right) + \frac{1}{r} k_f \frac{\partial}{\partial r} T_f + q_f = \rho_f c_f^p \frac{\partial}{\partial t} T_f \qquad (19)$$

with the following notations: r radius, T temperature, k thermal conductivity, q volumetric heat generation rate, t time, ρ density and c^p specific heat. This is the equation for heat conduction in the fuel neglecting axial heat conduction. The boundary conditions are

$$\left.\frac{\partial T_f}{\partial r}\right|_{r=o} = 0 \qquad (2o)$$

$$-k_f \left.\frac{\partial T_f}{\partial r}\right|_{r=r_f} = \alpha_{f,c} \left(T_f(r = r_f) - T_c(r = r_f)\right) \qquad (21)$$

where $\alpha_{f,c}$ is the heat transfer coefficient and r_f is the outer pellet radius.
k, ρ, c^p and α are temperature dependent and T is, of course, space and time dependent.

2. Can

$$\frac{\partial}{\partial r}(k_c \frac{\partial}{\partial r} T_c) + \frac{1}{r} k_c \frac{\partial}{\partial r} T_c + q_c = \rho_c c_c^p \frac{\partial}{\partial t} T_c \qquad (22)$$

This is the heat conduction equation for the can with the same notation as above. The boundary conditions are

$$\alpha_{f,c} (T_f(r = r_f) - T_c(r = r_f)) = -k_c \frac{\partial T_c}{\partial r}\Big|_{r=r_f} \qquad (23)$$

$$-k_c \frac{\partial T_c}{\partial r}\Big|_{r=r_c} = \alpha_{c,k} (T_c(r = r_c) - T_k) \qquad (24)$$

r_c is the outer can radius.

3. Coolant

Coolant behaviour is governed by the three equations for the conservation of mass, momentum and energy. By assuming an incompressible coolant and constant coolant velocity v_k, these equations reduce to the heat balance equation

$$\rho_k c_k^p \frac{\partial T_k}{\partial t} + v_k \rho_k c_k^p \frac{\partial T_k}{\partial z} = \frac{2\pi r_c}{F_k} \alpha_{c,k} (T_c(r = r_c) - T_k) +$$

$$+ q_k - \frac{F_s}{F_k} \alpha_{k,s} (T_k - T_s) \qquad (25)$$

$$T(z = z_o) = T_{in} \qquad (26)$$

where z_o is the position of the coolant entry, T_{in} coolant entry temperature, F_k is the free-flow area of the coolant and F_s is the wetted area of the structure material per cm of the coolant channel. With this equation the effects of friction and shockwaves can, of course, not be treated.

4. Structure material

Neglecting the heat conduction in the structure material, the following heat balance equation results:

$$\alpha_{k,s} (T_k - T_s) + q_s = \rho_s c_s^p \frac{\partial T_s}{\partial t} \qquad (27)$$

The temperatures T_k and T_s in equations (25) and (27) are functions of time and axial position. The parameters in all equations may be temperature dependent according to the following equations:

$$p(T) = p_1 + p_2 T + p_3 T^2 \qquad T < T^1$$

$$p(T) = p_4 \qquad T > T^1 \qquad (28)$$

Here, p denotes any of the parameters ρ, c, k or α, T is the temperature of the material involved and T^1 a limit temperature, i.e. melting temperature for fuel, can and structure material and boiling temperature for the coolant. α_{fc} is taken to be a function of the fuel temperature, $\alpha_{c,k}$ and $\alpha_{k,s}$ of the coolant temperature.

For the steady state reactor, eq.'s (19) - (27) apply with the time derivatives set equal to zero. The solutions for the steady state reactor serve as initial conditions for the transient equations. The calculation always starts with the evaluation of coolant and struture material temperatures and then, using the coolant temperature for the boundary condition, proceeds to the calculation of fuel and can temperatures. The Crank-Nicholson method is used for the solution of the heat conduction equations.

In its present form the thermodynamics module is incomplete in that it does not allow consideration of a number of important effects. Among these are

1. Treatment of a central hole in the fuel
2. Treatment of the gap between fuel and can with or without bonding
3. Time dependent coolant velocities and coolant entry temperatures.

These three effects will be included in the new thermodynamics module of RADYVAR, which will be inserted in KINTIC. In addition, coolant boiling is not accounted for in either of the modules. This will be treated by a new version of the BLOW-code /13/ to be incorperated later.

With the zone dependent temperature alterations, the feedback effects comprising Doppler cross section changes, density changes and zone volume expansion are calculated. For the cross section alterations due to Doppler effect, eq. (1)

$$\frac{\partial\sigma}{\partial T} = a\left(\frac{T_o}{T}\right)^x$$

is employed separately in each zone, using the mean fuel temperature alteration in this zone together with the parameters a, T_o and x pertaining to the material composition in the zone. a, T_o and x in one zone are, of course, given for each energy group and for capture and fission cross section separately.

The density changes of fuel, can etc. are computed using the temperature variation of each material in each zone and expansion coefficients for the different materials which may vary from channel to channel. The same expansion coefficients are used for computing the axial and radial expansion of each zone. The axial expansion is determined only by the axial expansion of the fuel and is therefore a function of the mean temperature alteration in the fuel $\overline{\Delta T_f} = \overline{T_f}(t + \Delta t) - \overline{T_f}(t)$ and the linear axial expansion coefficient of the fuel γ_f^{ax}:

$$\delta z = \overline{\Delta T_f}\ \gamma_f^{ax}\ \Delta z \qquad (29)$$

where Δz is the axial height of the zone at time t and δz its alteration. The radial expansion is determined by the deformation of the subassemblies, which are supposed to be fixed at the lower grid plate (at the coolant entry) and to have spacers in the middle of one axial zone. Therefore, the data of the structure material give the alteration of the radial dimensions:

$$\delta r = \Delta T_s\ \gamma_s^{ra}\ \Delta r \cdot G(z, \bar{z}) \qquad (3o)$$

where ΔT_s is the temperature alteration of the structure material in the zone, γ_s^{ra} is the radial expansion coefficient of the structure material and

$$G(z, \bar{z}) = 1 - 1.5 \frac{\bar{z} - z}{\bar{z}} + 0.5 \left(\frac{\bar{z} - z}{\bar{z}} \right)^3 \qquad z < \bar{z}$$

$$G(z, \bar{z}) = 1 + 1.5 \frac{\bar{z} - z}{\bar{z}} \qquad z > \bar{z} \qquad (31)$$

Here, z is the mean axial position of the zone and $\bar{z}$ is the axial position of the spacers. z = 0 is supposed to be the position of the grid plate.

The new zone dimensions are stored for each zone. For subsequent shape function calculations, the zones are forced into a rectangular grid by averaging in the radial and axial direction. This procedure clearly fails for bigger volume changes and will have to be replaced by a better method in the future.

VI. Description of external perturbation

As mentioned in the preceeding chapter, reactor perturbations originating from irregularities in the coolant flow cannot be treated by the present version of KINTIC. The perturbations that the code can handle must be caused by some sort of material movement in the reactor, e.g. control rod ejection. In reality, this means the continuous movement of a zone boundary through the reactor. One could think of realizing this directly in the code, but this method has not been adopted in KINTIC-1. Instead, the cross sections of the zone, through which the boundary moves, are changed gradually from one set to another during the time, in which the boundary is within the zone; e.g. in the case of a control rod ejection they are changed from the control rod mixture to the mixture of the follower. This is clearly an approximation to the true proceedings and may introduce a continuous over- or underprediction of the reactivity effect of the perturbation, as illustrated in fig. 3. There the true time dependent reactivity for, e.g. control rod ejection from the upper half of a core, is compared to the reactivity calculated by KINTIC with an axial subdivision of the upper core into two and four zones. One must clearly take care to make the zones which are affected by the perturbation sufficiently small.

Within the description adopted here, a perturbation is always reduced to the difference of two mixtures. These pairs of mixtures are defined in the NUSYS-part of the dynamics calculations already. In KINTIC-1, these mixture pairs are assigned the zones and time intervals during which they operate on the cross sections. By using the NUSYS-options for arbitrary changes of special cross sections one is able to create fictitions perturbations, e.g. growing fission cross section in one group and one zone.

Some examples of perturbations that can be simulated by KINTIC-1 are:

1. Control rod movement, ejection, insertion at predetermined times.
2. Movement of a sample, e.g. the boron sample in the superpromt critical experiment conducted on SEFOR.
3. Movement of a fuel rod or assembly, e.g. the accidental dropping of an assembly during reloading.

4. Fuel slumping, if a good model for the fuel movement exists. Feedback of temperature changes in the moving fuel on the movement cannot be incorporated, i.e. it must be estimated beforehand. In effect, fuel slumping is a feedback mechanism and will be incorporated as such in the future versions of KINTIC.

5. Sodium voiding. As in the case of fuel slumping, the time of the onset of boiling, the degree and speed of voiding must be determined beforehand. After the insertion of a voiding model, sodium void will be automatically treated as a feedback effect.

Though it is possible to treat these perturbation effects with KINTIC-1, one should remember that, at present, there is only one set of Doppler curves available for each zone. This means that the temperature dependence of the fission and capture cross sections is kept unchanged even if there are major cross section changes by perturbations. In perturbation cases 3 - 5, especially for sodium void, this is really not the case and one should use at least two sets of Doppler functions: One for the unvoided and one for the voided case. This should be kept in mind when calculating perturbations of types 3 - 5. A change of the program accounting for this effect will clearly have to be made - at the latest, during the insertion of a void module. As discussed below, the cross section concept used currently is under review now and will probably be altered; this affects the treatment of the Doppler effect.

VII. Method of solution; programs employed

In this chapter, some practical aspects of the method of solution are outlined. These are partly the result of the experience gathered already with the method. The realization of the code could in part be greatly simplified by employing already existing programs. These codes are listed below:

1. The multigroup diffusion program DIXY /1o/. The data management part of this program had to be slightly modified, but it is otherwise unchanged for the moment.
2. The perturbation routine which is originally part of the DIXY-package. Since the formulas for a perturbation calculation are very similar to those occuring in eq.s (11) - (13), the perturbation part of DIXY has been modified to give the point kinetics coefficients.
3. The point kinetics code AIREK /14/ for the solution of equations (7) - (8). This program has been modified to treat the time dependent coefficients ρ, β and l, which are given as second degree polynomials. The feedback equations, which form a part of the original AIREK version, have been deleted.
4. The thermohydraulics and feedback part of the older RADYVAR version /1/. Here, the program organization and data management had to be greatly modified so as to agree with the module and data transfer specifications given by the KINTIC-system, but the computational core of the program is unchanged.

During the development and tests of the code, a number of numerical difficulties have been encountered. Some of these are discussed here together with the method adopted to overcome them. One of the first difficulties related to the initial calculation of the reactivity which should be exactly zero for the steady state reactor, especially since ν is divided by k_{eff} after the steady-state criticality calculation to give an exactly critical system (see chapter III). Really, because of different formulas for the approximation of the diffusion operator and since the iteration process is never really completed, the reactivity will not be exactly zero. Originally, formula (13) was not used for the reactivity, but rather the following equation derived without using the adjoint equation (see chapter IV):

$$\frac{\rho}{l} = \frac{1}{I} \int_{Vol} \Big[\sum_g \psi^*_g \nabla D_g \nabla \psi_g + (1 - \beta) \sum_g \psi^*_g \chi_g \cdot$$

$$\cdot \sum_{g'} \nu\Sigma^f_{g'} \psi_{g'} + \sum_i \beta_i \sum_g \psi^*_g \chi^i_g \sum_{g'} \nu\Sigma^f_{g'} \psi_{g'} -$$

$$- \sum_g \psi^*_g \Sigma^{rem}_g \psi_g + \sum_g \psi^*_g \sum_{g'<g} \Sigma^s_{g' \to g} \psi_{g'} \Big] \qquad (32)$$

Theoretically, this formula gives the same value of the reactivity as eq. (13). In practice, the rounding-off errors falsify the result appreciably, ρ being the difference of nearly equal big numbers. Since the initial ρ was of the order of magnitude of several cents, formula (32) had to be eliminated in favor of (13), which reduced the initial error to 1 - 2 tenths of a cent. This is considered tolerable, as it does not induce a noticeable error into the transient.

Another difficulty was the initially very poor convergence of the multigroup diffusion routine for the inhomogeneous problem given by eq. (16). This could have been expected, since the largest eigenvalue of the corresponding homogeneous problem is nearly 1, and in such cases the source iteration method employed in DIXY is known to converge extremely slowly for the inhomogeneous problem. An analysis of the intermediate results indicated that the convergence of the flux shape was poor, whereas the amplitude very quickly reached the right value. It was therefore concluded, that instead of using the results of the foregoing flux shape calculation one had to employ a better first estimate. Now, if a new flux shape is to be calculated with eq. (16), the first step is the solution of the homogeneous problem, i.e. eq. (16) with all terms not containing ψ omitted. This solution normally takes only a few iterations. It is used as a first estimate for the solution of the inhomogeneous problem which then, in turn, needs only a few more iterations for convergence.

VIII. Time step automatization

A special effort has been devoted to the automatization of the time step determination (fig. 4). There are basically three levels of time steps pertaining to the different degrees of time dependence of the physical quantities. The flux amplitude varies the fastest and is therefore calculated using micro time steps, which are the steps employed in AIREK. A somewhat weaker time dependence is exhibited by the temperatures and therefore all feedback quantities. Recalculation of these quantities is therefore done only after a so-called normal time interval which comprises a number of micro steps. Normally, the most slowly varying quantity is the flux shape, which is recalculated only after one macro step consisting of several normal steps.

There are different criteria for determining the lengths of the time steps. AIREK contains a facility for automatic step length adjustment with upper and lower limits for the micro step length and the error criterion as input. The step length limits are internally prescribed by KINTIC, using $1o^{-7}$ sec, a value smaller than the average neutron lifetime for fast reactors, as the lower limit, and $1o^{-3}$ sec for the upper limit. The limits for the error criterion are external input, but recommendations as to their value are given in part 2 of this report. These recommended values have been arrived at by calculating the benchmark problem given in /15/ with AIREK and establishing safe values. As this benchmark problem puts much more stringent conditions on AIREK than any calculation in the framework of KINTIC has yet required, it is normally even possible to use larger error bounds whithout any loss of accuracy.

There are quite a number of criteria determining the length of the normal interval, which are listed below.

1. Reactivity criterion. If ρ_i is the reactivity at the start of the normal interval and ρ_f the reactivity at the end of the calculation and

$$\rho = \text{Max}\ (\rho_i, \rho_f);$$
$$d\rho = |\rho_i - \rho_f|,$$

the calculation is stopped for a new feedback determination if

1a: $\rho < .8\ \$$ and $d\rho > .5\ \$$

1b: $.8\ \$ < \rho < .95\ \$$ and $d\rho > .2\ \$$

1c: $\rho > .95\ \$$ and $d\rho > .1\ \$$

2. Time criterion. With Δt signifying the length of interval and l the neutron lifetime, the calculation is stopped if

$$\Delta t \geq 2 \cdot 10^{4}\ l$$

3. Minimax criterion: The normal interval ends when the flux amplitude reaches a minimum or maximum.

4. Amplitude criterion: The amplitude must not change by more than a factor of 10.

Criteria 2 - 4 are used only,if the amplitude has changed by more than 10 %.

5. Slope criterion: The time derivative of the amplitude must not change by more than a factor of 2. This criterion is only employed if the amplitude has changed by more than a factor 3.

6. The temperature change at any point in the reactor must not exceed 50 °C.

Criteria 1 - 5 are checked after each micro step.
Criterion 6 is tested after calculation of the feedback, i.e. after the normal step length has been determined by AIREK, and, if necessary, the normal step length is reduced for the inner iteration described below.

For the length of the macro interval, a test is made after each normal step for the maximum change of the contribution of each reactor zone to the reactivity. If this exceeds a value prescribed by the user a new shape function is calculated. Certain recommendations can be given as to the value of this limit, but it may change with the type of reactor.

The time dependent calculation is not straightforward but employs an inner and outer iteration which will be described now. As shown in chapter IV, the zero-dimensional part of KINTIC-1 uses time dependent coefficients ρ, β and l, the variation of which arises from two effects: The time dependence

of the cross sections, resulting from perturbation and feedback, and the time dependent shape function. The first kind of time dependence is treated in the normal time interval; the second one, in the macro interval.

When the calculation for a normal interval is started, certain guesses for the time dependence of the coefficients (due only to the cross section variations) are employed. Upon completion of the calculation for the normal interval, new values are obtained from the new temperature distribution. These new values normally deviate from the old ones and must, of course, be used as new guesses for the time dependence, and the normal interval must be recalculated. This constitutes the inner iteration. It is finished when the estimate of the point kinetics coefficients and their new values at the end of the normal step agree up to a small deviation specified by the user. For the reactivity, this is normally on the order of tenths of a cent. - The number of inner iterations necessary for convergence varies strongly with the feedback. As long as feedback plays no role in the variation of the cross sections, a few (1-3) iterations are sufficient. With strong feedback, many iterations, sometimes as many as 3o - 5o were necessary. To speed up the calculation, use has been made of the fact that in these cases the reactivity was observed to be oscillating about some intermediate value; after the first few oscillations, this value is internally estimated and used for the next iteration. This procedure brings the number of inner iterations for strong feedback down to 4 - 7. In some very rare cases, even this method does not ensure convergence; then, the time interval is halved after every 1o iterations until convergence is reached. With these procedures, no case has been found for which no convergence of the inner iteration could be obtained.

For the calculation of the point kinetics coefficients, the old shape function is used as long as it is the only one available. After evaluation of the new shape function, the coefficients are redetermined and may of course, exhibit some variations due to the new flux distribution. If these exceed some limits given by the user (e.g. some tenths of a cent for the reactivity), the whole macro interval is recalculated using for the time dependent shape function a linear interpolation between the two functions at the beginning and the end of the macro interval. This is the outer iteration. It may be repeated until convergence has been reached, but normally it is sufficient to recalculate the macro interval once without

doing a second shape function evaluation at the end of the calculation; sometimes even the recalculation of the macro interval proves unnecessary. All these determinations are made automatically by KINTIC-1.

The way, in which the perturbation time intervals are integrated into the automatic time scale is shown in fig. 4. Originally, there was only a prescription for the normal intervals, which could be part of only one perturbation interval. This must be postulated, because sudden changes in the mode of perturbation occuring at the boundary of a perturbation interval might provoke a break in the time dependence of the point kinetics coefficients which could not be satisfactorily represented by the quadratic interpolation used in the normal interval. Originally, no prescription was used for the macro interval, but now the same prescription is valid for the macro interval as for the normal interval. This has been deemed necessary from the following considerations: If the mode of perturbation varies strongly from one interval to another, the mode of shape function alteration will vary accordingly. For example, if an interval simulating a control rod extraction is followed by another one, in which no perturbation is present, i.e. with only feedback changes occuring, the shape function distortion will occur mainly in the first interval. In an outer iteration, on the other hand, the distortion would be spread equally over both intervals due to the linear interpolation between the shape functions, if a macro interval would consist of both or parts of both perturbation intervals. This would cause an error, which can only be avoided by prescribing a new shape function evaluation for each perturbation interval.

Though the course of the calculations is determined largely by the code, some of the criteria may vary with the type of reactor and are therefore left to the user. They are summarized here:

1. Micro step length criteria for AIREK. Recommendations are given in part 2 of this report, but larger limits may be employed.
2. Maximum ρ-, β- and l-deviation for inner iteration; for ρ a value of .3 cents is normally employed.
3. Maximum zonal alteration of ρ, β and l, used for determination of macro interval length; for fast reactors, 3o cents are used, but for another type of reactor and/or perturbation the optimum value may be different.

4. Maximum deviation of ρ for outer iteration, e.g. .5 cents.

5. Maximum number of shape function recalculations for outer iteration. Normally, this number is zero, in which case a recalculation of the macro interval is done if necessary, but the shape function at the end of each macro interval is calculated only once.

IX. Future developments

There are, of course, a number of physical effects occuring when an excursion passes the limits of the models contained in KINTIC-1. For these, calculational models have to be inserted in KINTIC. Apart from this, there are a number of improvements and extensions planned, which are listed here in random order:

1. The improved quasistatic method has to be introduced. In KINTIC-1, only slight changes have to be made for this except for the multigroup diffusion program DIXY, which in its present form admits only an external source of the form

$$Q(r,E) = \chi(E)\, q(r) \tag{33}$$

Even now, the source is not factorized in this way, but is (see eq. (16)):

$$Q(r,E) = \frac{1}{A} \sum_i \chi^i(E)\, \lambda_i\, C_i(r) \tag{34}$$

This is approximated, using an effective delayed spectrum $\chi_{eff}(E)$

$$Q(r,E) = \frac{1}{A}\, \chi_{eff}(E) \sum_i \lambda_i\, C_i(r) \tag{35}$$

thus arriving at the desired factorized form. For the improved quasistatic method, the term

$$\frac{1}{v(E)\Delta t} \cdot \psi\,(t - \Delta t, r, E)$$

is added to (34), making a factorization impossible. Therefore, DIXY must be extended to admit the most general form of external source which is the main task in connection with the improved quasistatic method.

2. Alteration of the cross section concept. The present method of treating the cross sections (one cross section set per zone) is adequate for the present model and in principle could be used with an extended model too, but would become very cumbersome for large material displacements. If the compositions undergo bigger changes, as must be anticipated for sodium void, fuel slumping etc., the microscopic effective cross

sections and the Doppler data change accordingly. One would therefore be forced to provide not one but several cross section sets for at least each core zone, e.g. for the voided and the unvoided case. Density changes would have to be inserted in all sets, multiplying the amount of work for cross section updating; the effective cross sections would have to be interpolated from the sets. Most important, the amount of storage at least on external units would be multiplied; internally it would be either multiplied too, or larger organizational changes would have to be made with a lot of additional data transfer. One must keep in mind that the cross sections even now occupy the largest amount of storage, e.g., in a typical 1500 mesh point - 6 group case the cross section region needs twice as much storage space as the shape functions. For a larger number of energy groups this factor would grow. If, additionally, several cross section sets per zone had to be stored, the resulting data sets would become unacceptably big. On the other hand, no use has been made of the fact, that many reactor zones have initially identical and later on similar compositions.

Preliminary investigations of effective microscopic cross sections and Doppler data as functions of fuel, coolant and structure material volume fractions have pointed out the need for composition dependent cross sections. An estimate has been made of the storage needed for such cross section sets, if these were stored not for each reactor zone but only for each block of zones with initially identical cross sections. In this case, the amount of storage would be nearly the same as with the present concept, but one would dispose of all data needed for treating even radical changes in compositions.Interpolation formulas for the changes in different volume fractions have already been developed.

A change of the cross section concept causes quite a number of changes in KINTIC-1 as well as in the NUSYS-programs and will therefore need some time. Up to now, no decision has been reached as to when this work will be started, but in view of the additional modules to be inserted (sodium void etc.) it seems to be undispensable.

3. Insertion of the modern version of the thermohydraulics module. This is being developed in the framework of a new version of RADYVAR and could be inserted upon its completion. Some adjustment of data transfer

to the KINTIC-1-specifications would have to be made. It is highly desirable to insert the new module, as it has been expanded to treat full or partial flow blockage, flow coastdown, temperature dependent gap between fuel and can and a central fuel hole.

4. Further expansions of KINTIC would be made for treating additional effects, i.e.

   a. Sodium void; later on it may become suitable to insert a two-phase flow boiling module for treating other coolants;

   b. Fuel element failure;

   c. Fuel slumping;

   d. Material redistribution;

   e. Fuel-sodium interaction;

   f. Core meltdown - second excursion.

   The methods for treating some of these effects are already being developed (sodium void, fuel element failure, core meltdown and second excursion). Fuel slumping probably presents no big problem. On the other hand, the work on models for material redistribution and fuel-sodium interaction is not so advanced. Even if all modules are available, the task of uniting them in one system, organizing automatic switches from module to module and finding the most effective mode for their interaction remains formidable. Presumably, this will be done in the framework of the new nuclear code system KAPROS which is presently at the Nuclear Research Center Karlsruhe.

The quasistatic method may quite easily be expanded to three dimensions. Nevertheless, such a program would reach the limits of present day computers. On the other hand, many perturbations can only be treated in three dimensions. At some future time, the feasibility of a three-dimensional version, e.g. in conjunction with the three-dimensional synthesis program KASY /16/ will be studied.

X. Results of calculations with KINTIC-1

In this chapter, some results of calculations done with KINTIC-1 are presented. These comprise preliminary calculations and comparisons as well as a study of the importance of space dependent effects for a prompt critical transient in SEFOR.

1. Comparison of asymptotic periods. The first investigation was concerned with the representation of asymptotic periods by KINTIC-1. One may calculate the reactor period analytically for only one group of delayed neutrons, solving the equations

$$\frac{dN}{dt} = \frac{\rho - \beta}{l} N + \lambda C$$

$$\frac{dC}{dt} = \frac{\beta}{l} N - \lambda C \qquad (36)$$

for known coefficients ρ, β, λ and l. The solution has the form

$$N(t) = a_1 e^{\omega_1 t} + a_2 e^{\omega_2 t} \qquad (37)$$

with, for ω_1 and ω_2

$$\omega_{1,2} = \frac{1}{2}\left(\frac{\rho - \beta}{l} - \lambda\right) \pm \sqrt{\frac{1}{4}\left(\frac{\rho - \beta}{l} - \lambda\right)^2 + \frac{\rho\lambda}{l}} \qquad (38)$$

The reactor period is $1/\omega_1$ with ω_1 containing the positive root.

The investigation was made with a very small bare cylindrical assembly (height 8o cm, radius 33 cm) and an overall perturbation, for which no space dependent effects were expected. Initially, the reactor contains equal amounts of ^{238}U and ^{235}U. The transients are induced by changing the ^{235}U-content. The multigroup calculations were done using two energy groups which were condensed from the 26-group ABN-set /7/. The data of the precursor group were β = .oo3, λ = .o8 sec^{-1} and energy spectrum equal to the prompt fission spectrum.

Three ways of calculating the reactor period or its equivalent, ω, were used. First of all, ρ and l were derived from two two-dimensional diffusion calculations with DIXY /1o/ for the perturbed and the unperturbed

assembly; with these and eq. (38), ω was evaluated. In the second method, KINTIC-1 was used to actually calculate the transient. The reactor was changed from its unperturbed to its perturbed state in .oo1 sec, and its behaviour was then followed until the asymptotic period was reached. The third value was again calculated from eq. (38), taking ρ and l from the asymptotic KINTIC-1 results.

The three values for ω as well as the different values for ρ and l are compared in table 1. One observes an excellent agreement of the periods derived directly from the flux behaviour in KINTIC-1 and from eq. (38) with the KINTIC-1 values. The agreement with the values based on the DIXY-calculations is very good too except for the nearly prompt critical case. There, very small errors in ρ(.5 %) and l(2.5 %) induce a big error in ω. As a systematic evaluation of eq. (38) has shown, this effect is characteristic for all cases with $\rho \approx \beta$. It underscores the need for a very accurate evaluation of ρ, l and β_{eff} for dynamic calculations. In our case, the difference was due to slightly different convergence criteria in DIXY and KINTIC-1 and to a small difference in the transport cross sections stemming from different condensation formulas.

Case		Eq. (38) with DIXY-results	KINTIC-1	Eq. (38) with KINTIC-1 results
Unperturbed reactor	l	$1.059 \cdot 10^{-7}$	$1.034 \cdot 10^{-7}$	
sub-critical	ρ	-.oo2121	-.oo2o98	
	ω	$-3.31 \cdot 10^{-2}$	$-3.3o \cdot 10^{-2}$	$-3.29 \cdot 10^{-2}$
supercritical, not prompt critical	ρ	.oo16o3	.oo16o2	
	ω	$9.18 \cdot 10^{-2}$	$9.16 \cdot 10^{-2}$	$9.17 \cdot 10^{-2}$
near prompt critical	ρ	.oo2918	.oo2932	
	ω	2.84	3.45	3.43
above prompt critical	ρ	.oo34o8	.oo3427	
	ω	$3.84 \cdot 10^{3}$	$4.13 \cdot 10^{3}$	$4.13 \cdot 10^{3}$

Table 1: Comparison of asymptotic periods for simple case

2. Comparison with results from the fully numerical code MITKIN. As a second test, KINTIC-1-runs were compared to results from the MITKIN-code /17/. All cases in ref. 17 have x-y geometry. Our first test involves test case 6 from ref. /17/, a two neutron group, one precursor group problem with a completely symmetrical square reactor, one quarter of which is shown in the upper right corner of fig. 5. The perturbation is induced in the zone marked by a P (and symmetrically in the other 3 zones not shown in the sketch) and consists of a ramp change of Σ_{capt} in group 2. The total change to Σ_{capt} in .2 sec is $\Delta\Sigma_{capt} = -.0035$. As this induced only a very mild transient, two additional calculations have been done with $\Delta\Sigma_{capt} = -.0070$ and $-.0090$, the third one leading to a prompt critical excursion.

The flux shape does not change appreciably for these cases. The biggest change occurs for the third case, for which the flux shapes are shown in fig. 5. The time dependence of the fast flux in the reactor centre is compared in fig. 6. Excellent agreement of MITKIN- and KINTIC-1-results can be observed for all three cases.

The computing times for MITKIN and KINTIC-1 were compared for all three cases on the IBM 360/85. They were nearly equal in the first case; in the second, the time needed by MITKIN was 2.5 times larger than the time used by KINTIC-1. In case three, this factor was 4.

Test case 8 from ref. /17/ is especially designed to result in time dependent flux shape alterations. Four energy groups and one delayed group with $\lambda = .08$ and $\beta = .0064$ are employed. The delayed spectrum is softer than the prompt fission spectrum, resulting in $\beta_{eff} = .0070$. The geometry is shown in fig. 7. Compositions 1 and 2 contain fissionable material with Σ_{capt} and Σ_{fiss} of composition 1 about twice as big as in composition 2. Σ_{fiss} is zero in composition 3. The transient is induced in the cross hatched region by changing the capture cross section in energy group 4 by $-.003$ in .2 sec.

It was not possible to work out a comparison between MITKIN and KINTIC-1 for this case which was entirely satisfying. The difficulties result from the different initial flux shapes calculated by the two codes. The original MITKIN case employs a very coarse mesh for this kind of problem (up to 20 mean free paths for some groups); DIXY and KINTIC-1 have to be run with only half of this step length for reasons of convergence and produce different initial fluxes. A sample of this may be gathered from table 2a and 2b, where

the spectra at point 1 and 2 as indicated in fig. 7 and the values of ψ(point 1)/ψ(point 2) are compared. The spectra turn out to be quite satisfying while the space distribution of the flux as represented by table 2b has an error of 2o % at these two points.

Additionally the attempt was made to run MITKIN with the same mesh as used by KINTIC, but in this case MITKIN develops instabilities which lead to meaningless results. It must be stressed here that the MITKIN version available in Karlsruhe dates from 1969 and that newer versions are probably improved in this respect. As a better version of MITKIN is presently not available in Karlsruhe, the comparison was done disregarding the initial flux shape differences, but no additional transients with steeper ramps were calculated.

	Point 1		Point 2	
Group	MITKIN	KINTIC-1	MITKIN	KINTIC-1
1	1.oo	1.oo	1.oo	1.oo
2	.91	.92	.99	1.oo
3	.62	.62	1.o8	1.11
4	.o8o	.o8o	7.19	7.83

Table 2a: Comparison of the spectra at point 1 and 2 of MITKIN test case 8. ϕ(group 1) has arbitrarily been set equal 1.

Group	MITKIN	KINTIC
1	3.41	4.o5
2	3.13	3.71
3	1.94	2.26
4	$3.79 \cdot 1o^{-2}$	$4.16 \cdot 1o^{-2}$

Table 2b: Values of ψ(point 1)/ψ(point 2) for all groups for MITKIN test case 8

Table 3 shows the values of $\phi(t = .3)/\phi(t = o)$ at the two points for all groups. As follows from the small reactivity addition ($\sim$ 13 ¢), the fluxes are not greatly increased, but the rate of growth is distinctly space- and energy dependent, with values varying between 13 % and 49 %. Despite the different shape functions, MITKIN and KINTIC-1 agree very well in the space and energy dependent growth rates.

	Point 1		Point 2	
Group	MITKIN	KINTIC-1	MITKIN	KINTIC-1
1	1.135	1.133	1.181	1.179
2	1.135	1.133	1.181	1.176
3	1.135	1.133	1.181	1.176
4	1.135	1.133	1.485	1.489

Table 3: MITKIN-test case 8. Comparison of $\phi(t = .3)/\phi(t = o)$ at point 1 and 2 for all energy groups

3. Comparison with TWIGLE. The last test case presented here can be found in a paper by J.B. Yasinsky /18/ (test geometry 2, problem 2). The geometry is that of a simplified PWR cylindrical reactor with inner and outer blanket, surrounding reflectors and one bank of partially inserted control rods. Two energy groups and one group of delayed neutrons are employed. The transient is induced by simulating a partial withdrawal of the rods. With a height of 28o cm and a 13o cm radius this thermal reactor is quite big if one keeps in mind that DIXY is essentially a code for fast reactors, which are much smaller in neutron mean free paths. Nevertheless, KINTIC-1 could easily handle this case employing only about 11oo mesh points; only the number of outer iterations in the diffusion calculations was distinctly bigger than for typical fast reactors.

In /18/, a comparison is made of a synthesized solution and the numerical solution employing TWIGL /19/. Fig. 8 shows the same comparison for the TWIGL- and KINTIC-1 solutions; it depicts the axial flux distribution in the inner blanket near the blanket-seed interface at different times. The agreement can be seen to be very good. The same holds for table 4, in

which the average flux rise taken from /18/ is compared to the amplitude A(t) from KINTIC-1.

Time [sec]	$\frac{\overline{\phi(t)}}{\phi(o)}$(TWIGL)	$\frac{A(t)}{A(o)}$(KINTIC-1)
o	1.oo	1.oo
.3	1.46	1.48
.4	1.95	2.o3
.5	3.58	3.56

Table 4: Comparison of flux rise for TWIGL and KINTIC-1 solution of thermal reactor test case.

4. Calculation of prompt critical transient in SEFOR. Recently, some calculations have been done for a prompt critical experiment in SEFOR. The main results are presented here.

The object of the calculations was an assessment of the importance of space-time dependent flux distributions for the evaluation of the experiment. For the relatively small SEFOR-core such effects were expected to be small. They were evaluated by running KINTIC-1 with the same thermodynamics parameters but with the different flux distribution options: Quasistatic, adiabatic and point kinetics.

The geometry of the SEFOR 1-D core is shown in fig. 9 /2o/. A prompt critical transient is induced by ejecting the boron absorber in the central channel. It is withdrawn in approximately 14o msec and has a total reactivity worth of 1.37 $, which is slightly bigger than the worth of the sample actually used (1.28 $).

The calculations were done using a 1456 point spatial mesh, 6 prompt and 6 delayed groups and 3 radial coolant channel segments with 6 axial zones for each. The 26-group-KFKINR cross section set /21/ was employed using two-dimensional spectra for group collapsing.

Fig. 1o shows the time dependence of the total reactivity (external perturbation + feedback) for the quasistatic approximation. The initial slope of the curve represents the acceleration of absorber motion. The reactor becomes prompt critical at about 8o msec and a slight secondary reactivity maximum occurs at 11o msec. The corresponding behaviour of the total power is shown in fig. 11. The maximum of power occurs at 87 msec. The experimental results display a power maximum of the same height about 1o msec later, which is in good agreement with this calculation, since the reactivity worth of the absorber is 1o ¢ higher in the calculations than in the experiment. - Fig. 12 shows the maximum central pin temperature in each of the three representative coolant channels.

Fig. 13 shows the radial flux distribution for some energy groups at the start and the end of the transient. The radial plane has been chosen to intersect with the initial absorber position. Obviously, the flux shape is affected only in the neighborhood of the absorber. This confirms the expectation that no appreciable space dependent neutron kinetics effects occur.

In order to confirm this, point kinetics calculations were done with KINTIC. This means, that the initial flux shape is not recalculated during the transient and it is used to determine the driving function and the power distribution. The time dependent power distribution, therefore, is the initial power distribution multiplied by the amplitude function as long as no feedback effects occur. Feedback, on the other hand, is calculated as before using the space dependent model. Therefore, when feedback effects become appreciable, the power distribution is affected by the space dependent fission cross section changes.

The results of the point kinetics calculations are shown in fig's 14 and 15. Three cases have been treated:

1. The shape function is the one corresponding to the initial reactor configuration with inserted absorber, and the reactivity is the one directly following from (13). It turns out that the slope of the reactivity is much too small with the maximum occuring at t = 1o4 msec as compared to t = 84 msec for the quasistatic case; no secondary maximum is observed (see fig. 14). The reason for this is, that eq. (13) is the formula resulting from first order perturbation theory for the reactivity, and in our case,

this is not sufficiently correct. This could be verified with static diffusion theory calculations, using perturbation theory and Δk_{eff}-calculations for the determination of the reactivity worth of the absorber.

2. Considering this effect, a correction factor f = Δk(exact)/Δk(perturbation) was calculated and used for the dynamics calculations. Again, the shape function is the one for the initial reactor configuration, but the reactivity resulting from eq. (13) is multiplied by f. In reality, only the driving function, i.e. the part of ρ resulting from the external perturbation should be corrected, but this could not be done, since the program only produces the total reactivity. Therefore the results become incorrect when feedback becomes appreciable and should not be compared for bigger time values.

   The resulting curve is much better (see fig.'s 14 and 15), but the maxima of reactivity and flux are 6 msec late, and the flux maximum is 24 % smaller than the quasistatic result. Seemingly the inital absorber effect is underestimated as it is moved out of a region with depleted flux and high importance without any correction for the flux depletion.

3. The method employed for the last calculation was the same as in case 2, but the shape function is the one corresponding to the final reactor state, i.e. with fully ejected absorber. The correction factor is defined as above, but, of course, has another numerical value corresponding to the different shape function. The initial temperature distribution corresponds to the final shape function, but turns out to be nearly identical with the initial distribution obtained with case 1 and 2. As can be seen from a comparison of fig.'s 1o, 11, 14 and 15, the results of this calculation are in excellent agreement with the quasistatic ones.

Finally, the effect of space dependent feedback was examined by comparing case 2 with the following case:

4. Shape function and reactivity correction were the same as in case 2, but with a zero dimensional feedback model. The thermodynamics parameters of all coolant channels are identical. In addition, the power distribution was averaged in all reactor zones, resulting in identical temperature values in all feedback zones. Instead of the composition dependent

curves for Doppler cross section changes, only one composition independent set of curves was used, which was calculated by weighting all sets with the zone volume and the mean flux pertaining to each composition. With this procedure, feedback becomes space independent.

With this model, the total reactivity becomes slightly bigger than the one in case 2 as soon as feedback becomes important. The flux maximum occurs at the same time, but is 1o % higher; for bigger times, the flux deviation goes up to 2o %. One must be very careful in interpreting these results, since, as shown above, the technique of correcting the total reactivity is in error when feedback becomes appreciable. Nevertheless, if the zero-dimensional feedback model would be correct, cases 2 and 4 should not deviate. The deviations are big enough to warrant further investigation with a zero-dimensional code employing externally determined driving functions, and, optionally, one- or several coolant channels like, e.g. FORE.

The following conclusions can be drawn from these results for the calculational analysis of the SEFOR-transient experiments:

1. Neutron Kinetics: A zero-dimensional model is very well suited provided that either the time dependent driving function is very carefully determined or the flux corresponding to the final reactor configuration (ejected absorber) is used for the determination of the driving function together with a time independent correction factor.

2. Thermodynamics and feedback: The need for a space-dependent treatment of thermodynamics and feedback is indicated. This should be further investigated with a zero-dimensional neutron kinetics code with an option for treating several coolant channels.

Some additional results from the calculations are

1. Adiabatic calculations have been done too, turning up no appreciable deviation from the quasistatic ones. The results are exactly those of fig.'s 1o - 12. This could be expected, since the transient is rather slow.

2. The neutron lifetime changes by .3 % during the transient with the maximum deviation occuring during the prompt critical interval.

3. Flux detectors were located in the outer reflector regions centrally below the core (boron-detector) and in the radial midplane (^{238}U-detector). The time dependent shape function alterations, i.e. the changes in the quotient of detector flux and total reactor power are 1.4 % for the axial and .9 % for the radial detector.

Concluding this chapter, one may state that KINTIC-1 is able to represent very exactly calculations done with numerical codes like MITKIN and TWIGL. It has proved to be an efficient and convenient tool for studies like the one done on SEFOR. The quasistatic calculation for SEFOR takes 9o min on an IBM 37o/165 with as much as 12 shape functions and 1 adjoint flux calcualtion. The point kinetics calculations take between 4o and 5o min, indicating that perhaps a speed-up of the perturbation calculation will have some effect on the machine time. This will be tried in the near future. All SEFOR calculations could be run without any external intervention in the automatic procedure, using error limits derived from foregoing fast reactor studies.

Part 2: Program description

I. Introduction

The second part of this report contains all information necessary for making calculations with KINTIC-1. As an introduction, the sequence of programs to be run is listed. It is assumed that steady state optimization studies for the reactor under consideration have been done already, that the reactor has a multiplication factor of about 1, and that space dependent condensation spectra from two-dimensional calculations are available, if needed. Then, the sequence of programs is as follows:

1. DOPKIN in conjunction with the NUSYS-programs for the evaluation of Doppler cross section derivatives. The card output of this run is inserted into the KINTIC-1 input stream.
2. NUSYS with special program 225o for cross section evaluation. Output of this run is a data set on tape or preferably disk for input in KINTIC-1. The KINTIC-1 run may directly follow this step.
3. KINTIC-1 step with card input partly derived from DOPKIN step and using the data set from the NUSYS/225o step. Optional output includes a data set, preferably a tape for evaluation runs.
4. Optional evaluation runs with DYNEVA, using the compilation of results produced and stored on tape by KINTIC-1.

The following three chapters contain the input descriptions and lists of control cards for DOPKIN, 225o, and KINTIC-1 including the ASP-control cards necessary for the ASP-operating system which is currently used in Karlsruhe. Then, the input list is given for a small sample case. Chapter VI contains some information on the internal structure of KINTIC-1, including flow-charts of the control program.

II. Input and control cards for DOPKIN-job

This chapter and the following one contain frequent references to the Karlsruhe nuclear code system NUSYS. It is assumed that the user is acquainted with the basic nuclear data evaluation programs in this system, e.g. the cross section determination program 446 and the condensation program 352, as well as with the utility program 451.

Presently, DOPKIN is not completely integrated into NUSYS, but exists as a card package which has to be compiled and linked to NUSYS for every DOPKIN-run. This presents no great inconvenience since DOPKIN-runs are quite rare compared to the frequency of KINTIC-runs. For users, the card package is available from the authors.

One or two data sets must have been created in the NUSYS data file before starting DOPKIN. These are the KØMPØ block which contains all information on the compositions and the cross section set to be used and, if group collapsing is required, the SPEKT block with the condensation spectra. The sequence of NUSYS programs is therefore

1. NUSYS start-up program 397
2. NUSYS utility program 451 for bringing the blocks KØMPØ and SPEKT into the NUSYS data file
3. DØPKIN, which is informally assigned the program number 99997

Alternately, if the user is interested in the macroscopic cross sections, he may use 451 only for bringing the SPEKT block into the data file and then call the cross section program 446, before starting DOPKIN. In addition to calculating the cross sections, 446 can be used to store the KØMPØ block in the proper from.

DOPKIN needs the multigroup cross section sets, e.g. the 26 group KFKINR set and the Karlsruhe nuclear data file KEDAK in addition to the one or two data blocks. With this and a small card input it does the following calculations:

1. Internal subdivision of all compositions into groups of compositions. This is necessary because the NUSYS Doppler program can handle only a limited number of compositions, which may not differ too much in enrichment.

2. Alteration of fuel density due to the fuel temperature, for which the Doppler derivatives are to be calculated.

3. Automatic call of the NUSYS Doppler program for each group of compositions and each temperature.

4. After each call, automatic storage of the derivatives calculated by the Doppler program.

5. After all derivatives have been calculated, optional group collapsing.

6. Then, a least squares fit is made for each (collapsed) group and each mixture, which results in the parameters a and x of the approximation function

$$\frac{\partial \sigma}{\partial T} = a \left(\frac{T_o}{T} \right)^x \qquad \text{(see eq. (1) in part 1)}$$

The parameters a, x and $T_o = 300^oK$ are punched for each mixture and each group in the order given by the KØMPØ block.

For these operations, the card input must contain the following information:

1. The temperatures at which the Doppler derivatives shall be calculated.

2. Coefficients of polynomials giving the fuel density variation with temperature. The density is assumed to vary as

$$\rho = \rho_0(1 - 3\gamma(T))$$

with

$$\frac{d\gamma(T)}{dT} = P_1 + P_2 T$$

ρ_0 is the density at 293°K, and it is assumed that the initial compositions as given in the KØMPØ block pertain to this temperature. P_1 and P_2 are card input. As they are the same for compositions with similar enrichments, only a limited number of such polynomials are input together with numbers appointing the adequate polynomial to each mixture.

3. Group collapsing information, if needed.

The input has the normal NUSYS-format, i.e. it is unformatted. It is listed here in the usual NUSYS notation with Kn signifying a new card and Sn signifying a logical decision. New cards must have some non-blank sign in the first column; continuation cards must begin with a blank. Variable names starting with I-N indicate fixed point numbers, all others are floating point numbers.

Input-list for DØPKIN:

K1	Ø99997Ø	constant
K2	NTEMP	number of temperatures to be calculated (≤ 15)
	(TEMP (I), I=1,NTEMP)	temperatures /°K/

K3	NPØLY	number of expansion polynomials (≤ 6)
	(P1 (I), P2 (I), I=1, NPØLY)	P_1, P_2 for each polynomial (see above)
K4	(MIPØL, (I), I=1, MI)	for each composition, number of the adequate expansion polynomial . MI is the total number of compositions as given by the KØMPØ-block.
S5	for group collapsing continue with K6-K7, else K8	
K6	∂CØND∂	constant
K7	NGG	new number of groups
	(NGRGR (I), I=1, NGG)	for each new group, number of the last old group it contains (as in group collapsing program 352)
K8	NUFIN	constant; end of input.

This input follows the input for the foregoing NUSYS-programs, e.g. 397 and 451 in the sequence cited above. In the card input of the program directly preceding DOPKIN, the number 99997 must be assigned as the number of the following program.

Among the control cards needed for a DOPKIN run on the IBM 370/165 are the cards providing the nuclear data sets and control cards for the step linking DOPKIN into the NUSYS-system.

Control cards for DOPKIN-job:

```
// Usual job-card with REGIØN = 300K
// EXEC FHCLG,LIB=NUSYS,PARM.L='ØVLY'
// PARM.G=170000
```

```
//C.SYSIN DD *
    DOPKIN card deck
//L.SYSUT1 DD SPACE=(3303,(400,20),UNIT=DISk
//L.SYSLMØD DD UNIT=DISK,SPACE=(3303,(400,20,1),RLSE)
//L.SYSPRINT DD SPACE=(TRK,30)
//L.SYSIN DD *
  INCLUDE LØAD(ANUSY)
  INCLUDE ØBJ(PNUSY)
//G.FTO7FOO1 DD SYSØUT=B
/*FØRMAT PU,DDNAME=FTO7FTOO1,FØRMS=STANZ
//G.FTO1FOO1 DD DSN=KNDF,UNIT=2314,VØL=SER-NUSYS1,
// DISP=SHR
//G.FTO4FOO1 DD DSN=GRØUCØ,UNIT=2314,VØL=SER=NUSYSO,
// DISP=SHR
//G.FTO8FOO1 DD UNIT=DISK,SPACE=(TRK,10)
//G.SYSIN DD *
    Input for NUSYS programs ending with DOPKIN-input
//  "end of job" card                                    //
```

DOPKIN output is a printed output with all intermediate results and the punched cards. Each card contains first the temperature T_o = 300 °K, then x_f, x_c, a_f and a_c for fission and capture cross section for one group and one composition. For each composition NGG cards are punched. If in KINTIC-1 one composition turns up in more than one coolant channel, one must duplicate the corresponding cards, as each channel needs its own Doppler data sets (see KINTIC-1 input). Apart from this sorting process and establishing the correct correspondence between Doppler data and compositions in each coolant channel, the punched cards may be directly inserted into the KINTIC-1 card input.

A DØPKIN-run with 26 groups, 10 mixtures and five temperatures takes about 1 min. on the IBM 370/165.

III. Sequence of NUSYS-programs for cross section evaluations, input for 2250, and control cards

The NUSYS job step for evaluating the cross sections for the kinetics calculations must perform the following tasks:

1. Evaluation of the isotope dependent cross sections for all compositions in e.g. 26 groups
2. Optionally evaluation of condensation spectra and group collapsing.
3. Duplication of compositions, if the reactor contains zones with initially identical compositions (see chapter II.1 of part 1)
4. Calculation of the macro-material cross sections, i.e. the cross sections pertaining to fuel, can, coolant, structure material and optionally bonding from the isotope dependent cross sections (see chapter II.1 of part 1)
5. Incorporation of the delayed neutron data into the cross section blocks
6. Inclusion of the perturbation data
7. Transformation of data block structure and creation of the external data set for KINTIC-1

The first two items of this list are carried out by the common NUSYS-routines for cross section evaluation; whereas, for the following tasks, a special program 2250 has been written. 2250 is called at the end of the cross section evaluation step and needs as input:

1. the KØMPØ block for all compositions
2. the SABBR cross section block containing the isotope dependent cross sections with the following types: CHI, NUSF, SCAPT, SFISS, SMTØT, SREM, STR, 1/V

3. a card input containing information on
   a. the numbers of compositions to be duplicated and the number of times that the duplication is to be made,
   b. the precursor groups,
   c. the decomposition of the compositions into macro materials,
   d. the perturbation.

Before giving an input description of 2250, some examples of program sequences will be presented. Of course, there is a number of possibilities for creating the necessary data before starting 2250. The easiest one is a card input of the cross sections, which is often used for test cases. The sequence of NUSYS modules is then:

1. 397 NUSYS startup routine
2. 451 NUSYS utility program for bringing the blocks KØMPØ and SABBR into the NUSYS data file
3. 2250

If the cross section sets are to be used for creating the nuclear data, one has to call the programs 446 and, usually, 352. For a common case needing 10 - 30 different compositions and starting from a 26 group cross section set, it is not possible to calculate the cross sections for all compositions and all isotopes in one step, because the necessary main storage is far too big. Therefore, the compositions have to be subdivided into groups of 3 - 7 depending on the number of isotopes, groups and the available core memory, and the cross section evaluation and collapsing process has to be made for each of these groups seperately. The results of each step are stored externally and, at the end of the calculation, the program 2291 is used to join all intermediate results in one block. Some rules should be observed in this case:

1. The KØMPØ blocks of all composition groups must contain the same isotopes in the same order.

2. Each composition group should contain at least one core mixture, whose spectrum is to be used for collapsing the inverse group velocities. Otherwise, appreciable errors in the neutron lifetime may occur.

3. If $\beta_{eff} \neq \beta$, i.e. if the delayed and the prompt neutron spectra differ, the first composition in the first composition group should be a core composition.

Two examples for the sequence of NUSYS modules for a cross section evaluation using a 26 group set with collapsing are given below. In the first case, the spectra for condensation have been derived from a two-dimensional steady-state calculation and are card input:

1.	397	NUSYS startup routine
2.	446	NUSYS cross section evaluation module for creation of 26 group cross sections for composition group 1. Output: 26-group SABBR block, KØMPØ block and SIGMA block
3.	352	NUSYS group collapsing module. Output: Collapsed SABBR block; old SIGMA and SABBR block is deleted.
4.	451	NUSYS utility module for writing the KØMPØ block and the collapsed SABBR block into external file.
5.	397	NUSYS startup routine for deleting KØMPØ and SABBR block
6.	ff	repeat sequence 446/352/451/397 for all composition groups
7.	2291	NUSYS program for reading the external file created by 451 and collapsing all SABBR blocks into one SABBR block and likewise all KØMPØ blocks
8.	2250	

The third example differs from the second one in that the collapsing spectra are to be calculated by the one-dimensional diffusion routines contained in NUSYS. It is assumed that all necessary spectra may be derived from one one-dimensional calculation

1.	397	NUSYS startup routine
2.	446	NUSYS cross section evaluation routine for those compositions needed for the one-dimensional 26 group diffusion calculations. Output: 26 group SIGMA block
3.	6731	NUSYS 1d diffusion module for calculating k_{eff} and 1d-26 group flux distribution . Output: FLUX1 block containing the flux distribution and GEØ block containing the 1d geometrical configuration
4.	2731	NUSYS 1d evaluation program for calculating zone averaged spectra. Output: SPEKT block containing the spectra. The FLUX1, GEØ and SIGMA blocks are deleted
5.	ff	program sequence 446/352/451/397 for all groups of compositions as in the foregoing example. In 352, the spectra are taken from the SPEKT block created by 2731 instead of being card input. With the last call to 397, the SPEKT block should be deleted.
6.	2291	NUSYS module for joining all SABBR and KØMPØ blocks (see above)
7.	2250	

Other examples for the cross section evaluation, whose module sequence the user may easily construct, are: Same procedure as in the third example, but using spectra from an axial one-dimensional calculation for one part of the compositions and those

from a radial calculation for the other part; or: Cross section evaluation for a two-dimensional 26 group diffusion calculation in a first NUSYS jobstep; two-dimensional 26 group diffusion calculation and evaluation in a DIXY jobstep, using the cross sections from the foregoing jobstep; second NUSYS jobstep, using the DIXY-results for creating a SPEKT block with two-dimensional collapsing spectra and then evaluating the cross sections for the kinetics run.

After these more general remarks, we can now give the lists of card input for 2250 and the control cards for the NUSYS jobstep. Unlike DOPKIN, 2250 is integrated into the NUSYS system, i.e. it can be called by setting the number of the following module equal 2250 in the card input of the preceding module

Input list for 2250:

K1	∂02250∂	constant
K2	2290	"
	NG	number of energy groups (≤ 26)
	MI	number of compositions in the KØMPØ block
	NMW	number of original compositions to be duplicated for use in KINTIC-1
S3	if NWM=0	continue with K5, else with K4
K4	(NID(I), NM1(I), NM2(I), I=1, NMW)	the number of compositions is enlarged in the following way: Compositions NM1(I) through NM2(I) are identical to composition NID(I). For I=1, NM1(I) must equal MI+1; for I ≠1, NM1(I) = NM2(I-1)+1.
K5	NBETA	number of precursors (≤6)
	MBETA	number of heavy isotopes producing delayed neutrons
S6	for each precursor K7	
K7	(CHID(I), I=1, NG)	group dependent delayed neutron spectrum

S8	for each of the MBETA heavy isotopes K9	
K9	NAME	name of the isotope as given in the KØMPØ block (e.g. ∂U235O∂)
	(BETA(I), I=1,NBETA)	fraction of precursors produced in fission for each precursor group
	(XLAM(I), I=1,NBETA)	decay constant for each precursor group
S10	for each of the MI original compositions K11 - K13	
K11	NAK	number of macro-materials in the composition (≤ 5). Normally NAK=1 for compositions in non-feedback-zones and NAK=4 or 5 in feedback zones
S12	for each macro-material in the composition K13	
K13	LABEL	name of the macro-material. Possible names: ∂BRENN∂ for fuel, ∂HUELL∂ for can, ∂KUEHL∂ for coolant, ∂STRUK∂ for structure material and ∂BØNDI∂ for bonding. The macro-material BØNDI may be used for gathering contributions, which for some reason should not turn up in the other macro-materials
	NIS	number of isotopes contributing to the material
	(NAMIS(I), FRACT(I), I=1,NIS)	For each isotope: Its name as given in the KOMPØ block, e.g. ∂AL27O∂; the fraction of its concentration contributing to the macro-material, i.e. $0 \leq$ FRACT(I) ≤ 1. The sum of the fractions of each isotope in all macro-materials pertaining to one composition must equal 1
K14	NPER	number of composition pairs for definition of external perturbation ($1 \leq$ NPER ≤ 20)
S15	for each composition pair K16	

K16	NMST1 NMST2	the perturbation in one zone and one perturbation time interval consists in replacing composition NMST1 by composition NMST2. If the pair NMST1 and NMST2 is the same for N zones, they must be defined N times
S17	NUFIN	constant; end of card input.

As already mentioned, 2250 creates an external data set for use with KINTIC-1. This is normally assigned some name and stored in some library. The control cards for the NUSYS-step contain, therefore, first the cards for a utility step deleting any duplicate data set from the library, in case an older data set exists with the same name. After this follow the control cards for the real NUSYS jobstep, among them: one card providing the 26 group cross section set, one for the intermediate data set used for storing the KØMPØ and SABBR blocks for the individual composition groups, which, of course, can be deleted for example 1, and one for the resultant KINTIC-1 data set.

A list of job control cards is given here for an example with 25 original compositions, 46 total compositions (including the duplicated ones), 6 energy groups, 6 precursor groups and 15 isotopes. The composition groups contain up to 6 compositions resulting in a main storage of 700 K bytes. This job takes about 14 min. on the IBM 370/165.

Job control cards for the NUSYS-jobstep

```
// Usual job card with REGIØN=700K
// EXEC PGM=IEHPRØGM
//SYSPRINT DD SYSØUT=A
//A1 DD DSN=dsname,UNIT=2314,VØL=SER=dkname,
// DISP=(ØLD,DELETE)
//SYSIN DD DUMMY
// EXEC FHG,LIB=NUSYS,NAME=ANUSY,REGIØN.G=700K,
// PARM.G=578000
//G.FT04F001 DD DSN=GRØUCØ,UNIT=2314,VØL=SER=NUSYS0,
```

```
// DISP=SHR
//G.FT08F001 DD UNIT=DISK,SPACE=(TRK,10)
//G.FT15F001 DD UNIT=DISK,SPACE=(TRK,50)
//G.FT20F001 DD DSN=dsname,UNIT=2314,VØL=SER=dkname,
// DISP=(NEW,KEEP),SPACE=(TRK,25)
//G.SYSIN DD *
    NUSYS-input cards
//  "end of job" card                                    //
```

In this list, dsname is the symbolic name of the KINTIC-1 data set and dkname is the name of the library, into which the data set is delivered. Furthermore, the data set reference number of the intermediate data set has been assumed to be 15, that of the KINTIC-1 data set to be 20.
Note: The release-option should not be used with the KINTIC-1 data set. Rather, the user should try to make a good estimate of the space needed and check afterwards the number of tracks actually needed.

Instead of fishing the job, the user may directly continue with the KINTIC-1 job step. If the data set is to be reserved for a larger number of KINTIC-1 calculations, this first KINTIC-1 calculation must be preceded by the job steps for copying the KINTIC-1 data set, which will be described in the next chapter. For big reactors, it is preferable to have two jobs, as the NUSYS-step needs comparably small computer time and a large amount of storage, whereas the KINTIC-1 step needs larger computer times and a smaller memory.

IV. KINTIC-1 input, control cards and output

This chapter gives all information needed for the real KINTIC-1 run, including a short listing and explanation of the necessary input data, the input list, control cards and output description. The input of KINTIC-1 comprises the following data:

1. The KINTIC-1 cross section set from a foregoing NUSYS-run
2. Control data, partly for internal data management, but mainly for controlling the calculation
3. Definition of the perturbation
4. Data concerning the initial reactivity iteration
5. The total initial power and the zone dependent fuel volume fractions for the calculation of power distribution
6. Input for DIXY consisting mainly of the reactor configuration

The input is unformatted with the exemption of the DIXY input which retains the original formatted input. An important relation exists between the DIXY input and the feedback part of the program, when feedback is used. In the feedback input, only NKKN, the number of radial segments used for the definition of the characteristic coolant channels and NM, the number of axial zones per segment are given. The location of the zones assigned to each channel is given by the DIXY input via the following prescription:

1. Contrary to the original DIXY input specifications, overlay of region input is not admissible.
2. In the order of DIXY zone definitions, the first NKKN·NM zones must be the coolant channel zones. After these, further non-feedback zones like reflectors or control rod zones may be defined in arbitrary order.
3. Among the feedback zones, the first NM zones are those pertaining to the first radial segment, the next those for the next segment etc.

The NM-zones pertaining to one segment must be ordered according to the direction of the coolant flow, i.e. the first one must contain the coolant entry, the last one the coolant exit. The distribution of axial zone heights may be chosen freely in the first radial segment. All other segments must have the same distribution.

As the total input list is quite long it is given here in three parts. The first one is the basic KINTIC-1 input without feedback and DIXY-input. Second, the thermodynamics and feedback input, which is the largest part, is given. Then, the DIXY-input is listed. It is nearly identical with the original DIXY-input, but since only the input for the DIXY diffusion calculation routine is needed and since some variables in the original DIXY input must be assigned special values for use with KINTIC-1, we have preferred to submit a special listing. The three input parts are linked in the following order: One starts with the basic KINTIC-1 input, inserting the feedback input near the end at the location indicated in the listing. Then the DIXY-input follows the basic KINTIC-1 input.

Basic input for KINTIC-1

K1	$START$	constant
K2	NG	number of energy groups (≤ 26)
	NV	number of precursor groups (≤ 6)
	NZ	number of DIXY-zones (≤ 100)
	NPKT	number of space points
	NKKN	number of radial segments ($0 \leq NKKN \leq 10$)
	NM	number of axial zones for each segment ($0 \leq NM \leq 10$)
	NNMAX	maximum number of radial zones in the fuel for temperature distribution ($0 \leq NNMAX \leq 6$)
K3	NAUS	= 1 Maximum KINTIC output for code testing

		= -2 big output = -1 medium output, with shape function = 0 small output, without shape function The tape output for DYNEVA is uninfluenced by NAUS
	KTPØUT	> 0 data set reference number for storage of tape output ($1 \leq KTPØUT \leq 99$; $KTPØUT \neq 5,6,7,20,21,22$) = 0 no tape output
	XLABEL	16 alphanumerical characters as label for the DYNEVA data file, e.g. 'NA2 CASE 8 EPS-4'
K4	$PERTUR$	constant
K5	NST	number of time intervals used for definition of the perturbation
S6	for each perturbation time interval K7	
K7	NL	number of following data = 2·NZST+2
	TST	end of perturbation interval (sec). It is assumed that each perturbation interval starts at the end of the foregoing interval; the first one starts at t = 0.
	NZST	number of perturbed zones in this interval
	(NS(I), NMI(I), I=1,NZST)	for each perturbed zone: number NS of perturbation composition pair in the order of cards K16 of the 2250 input; composition number NMI of the perturbed zone
K8	$CØNTRØL$	constant
K9	NIT	number of shape function iterations (normally 0)
	KZERØ	0 quasistatic or improved quasistatic method 1 point kinetics -1 adiabatic method

	CØRR	correction factor for ϱ for KZERØ=1 CØRR=1.: no correction
	KQB	0 quasistatic method 1 improved quasistatic method (not yet available in August 1972; for later information please contact authors)
K10	EPS1	lower limit for accuracy test for point kinetics module; recommended value 10^{-5}
	EPS2	upper limit for accuracy test for point kinetics module; recommended value 10^{-4}
	EPS3	maximum deviation of reactivity at the end of a macro interval /$\bar{\$}$/
	(EPS4(I), I=1,NV+2)	maximum deviation of reactivity ϱ, lifetime l and β_i^{eff} at the end of a normal interval /$\bar{\varrho}$: absolute value, i.e. $\Delta\varrho_{max}$; l, β_i^{eff} relative value, i.e. $\Delta l_{max}/l$ etc./
	(EPS5(I), I=1, NV+2)	maximum alteration of ϱ, l and β_i^{eff} in each reactor zone during one macro interval /$\bar{\varrho}$: absolute value; l, β_i^{eff} : relative value/ These quantities regulate the length of the macro interval. Recommended values for fast reactors: $\varepsilon_5(\varrho) = .001$; $\varepsilon_5(l) = \varepsilon_5(\beta) = .1$
K11	ØPØWERØ	constant
K12	XP	initial reactor power /$\bar{M}\ \bar{W}$/
K13	ØØMEGAØ	constant
K14	(OM(I), I=1, NZ)	for each zone in the order given by the DIXY input its fuel volume fraction
S15	if the calculation is to proceed to its end K16, otherwise K18	
K16	ØENDEØ	constant
S17	proceed with K20	

K18	§CHECK§	constant
K19	NCHEC	1 checkpoint after consistency and k_{eff}-iteration
		2 checkpoint after thermodynamics calculation for steady state reactor
		3 checkpoint after MAKMAX macro intervals
	MAKMAX	number of macro intervals before checkpoint
K20	§CØNSIS§	constant
K21	KØNSI	1 consistency iteration for cross sections; cross sections and densities are made consistent with temperature distribution
		-1 consistency iteration for cross sections only
		0 no consistency iteration
	KØNE	1 k_{eff}-iteration, if KINTIC-1 options are to be used (see part 1, chapter III,2)
		0 otherwise
	EPS6	maximum deviation of k_{eff} from 1 for KØNE=1
K22	ff insert input for thermodynamics and feedback part	
S23	if KØNE ≠ 0 go to K24 ff, else proceed with K29	
K24	ANA	§RADIT§ k_{eff} is adjusted by enlarging or contracting the reactor
		§MATIT§ k_{eff} is adjusted by changing compositions
S25	if ANA=§RADIT§ proceed with K26, otherwise with K28	
K26	ALPH1	'HSTP' if horizontal reactor axis is to be changed
		'VSTP' if vertical reactor axis is to be changed
	FACT	initial reactor dimension l is varied in the limits l·FACT and l/FACT

S27	proceed with K29	
K28	NNMI	number of compositions that are to be changed
	(NUMI (I), I=1,NNMI	numbers of these compositions
	ALNAM	name of the macro material which is to be changed (ØBRENNØ, ØHUELLØ etc. according to K13 in input for 2250)
	FACT	the cross sections σ of the macro material ALNAM in the NNMI compositions are varied in the limits σ ·FACT and σ/FACT
K29	ØFØRMØ	constant
K30 ff		formatted DIXY input
S31	end of total input	

Input for thermodynamics and feedback part

K1	ØFEEDBACKØ	constant
K2	NKKN	number of radial segments for the definition of coolant channels ($0 \leq NKKN \leq 10$)
	NM	Number of axial zones per segment ($0 \leq NM \leq 10$)
	NNMAX	maximum number of radial zones in fuel pellet ($0 \leq NNMAX \leq 6$)
	KENBØ	= 0 (option for special treatment of bonding; currently not in use)
	NVØIN	0 no volumetric changes calculated 1 volumetric changes are taken into account

	NPRINT	regulates the thermodynamics and feedback output for the instationary calculation, if NAUS (K3 of basic input) $\neq$ 0 or - 1:
		- 2 shortened output after each normal interval iteration
		- 1 extensive output after each normal interval iteration
		0 no output
		1 output only at perturbation interval ends
	NSTUE	number of axial zone containing the spacers.
	NFEED	0 no thermodynamics and feedback taken into account
		1 calculation with feedback (only for rz - geometry)
	1	constant
S3	for NFEED=0 end of feedback input; else proceed with S4	
S4	for each radial segment K5 - K9	
K5	KKN	number of the segment
	VSTRUC	volume fraction of the structure material /cm^3/
	NN	number of radial zones in the fuel ($2 \leq NN \leq 6$)
	RBR	pellet radius /cm/
	DCAN	can thickness /cm/
	RKUE	equivalent radius of coolant channel /cm/
	VDUF	quotient of volume of structure material / the part of its surface which is in contact with the coolant /cm/
	DELTB	estimate of radial temperature difference in the fuel /°C/

EPSK	accuracy limit for temperature iteration /°C/; recommended value .01
VKUEL	coolant velocity /cm/sec/
TKIN	coolant entry temperature /°C/
ANTB	fraction of heat released in fuel
ANTC	fraction of heat released in can
ANTK	fraction of heat released in coolant
ANTS	fraction of heat reieased in structure material
TSBR	fuel melting temperature /°C/
TSCAN	can melting temperature /°C/
TSKUE	coolant boiling temperature /°C/
TSSTR	structure material melting temperature /°C/
UMELT	fuel melting heat /cal/cm^3/
URECR	fuel recristallization heat /cal/cm^3/

K6 this card contains the temperature dependent thermodynamics parameters in the form p (1), p (2), p (3), p (4) (see eq. (28)). The parameter p as a function of temperature T is

$$p(T) = p(1) + p(2)T + p(3)T^2 \quad \text{for } T < T_{limit}$$

$$p(T) = p(4) \quad \text{for } T > T_{limit}$$

T_{limit} equals TSBR, TSCAN, TSKUE or TSSTR according to the temperature on which p depends.

(RØB (I),I=1,4)	fuel density /g/cm^3/; function of T_f
(RØC (I),I=1,4)	can density /g/cm^3/ ; function of T_c
(RØK (I),I=1,4)	coolant density /g/cm^3/; function of T_k
(ROS (I),I=1,4)	structure material density /g/cm^3/; function of T_s
(CPB (I),I=1,4)	specific heat c_p of fuel /cal/(g $^\circ$C)/; function of T_f
(CPC (I),I=1,4)	specific heat c_p of can /cal/(g $^\circ$C)/; function of T_c
(CPK (I),I=1,4)	specific heat c_p of coolant /cal/(g $^\circ$C)/; function of T_k
(CPS (I),I=1,4)	specific heat c_p of structure material /cal/(g $^\circ$C)/; function of T_s
(HBC (I),I=1,4)	heat transfer coefficient fuel-can /cal/(cm^2 sec $^\circ$C)/; function of T_f
(HCK (I),I=1,4)	heat transfer coefficient can-coolant /cal/(cm^2 sec $^\circ$C)/; function of T_c
(XLB (I),I=1,4)	fuel heat conductivity /cal/(cm sec $^\circ$C)/; function of T_f
(XLC (I),I=1,4)	can heat conductivity /cal/(cm sec $^\circ$C)/; function of T_c

K7	KKN	number of the segment
	MD	number of different sets of following data
	(ALPHA(I),	coolant volume fraction
	BETAAB(I),	spacer volume fraction
	BETAKA(I),	volume fraction of subassembly walls
	E(I),	clearance between fuel and can /cm/
	I=1,MD)	

	(MZ(I), I=1, NM)	each axial zone is assigned one of the data sets (ALPHA, BETAAB, BETAKA, E) according to the value of MZ
K8	KKN	number of the segment
	AUSBAX	linear axial expansion coefficient for fuel (1/ ^{o}C)
	AUSCAX	linear axial expansion coefficient for can (1/ ^{o}C)
	AUSSAX	linear axial expansion coefficient for structure material (1/ ^{o}C)
	AUSBON	volumetric expansion coefficient for bonding (1/ ^{o}C)
	AUSBRA	linear radial expansion coefficient for fuel (1/ ^{o}C)
	AUSCRA	linear radial expansion coefficient for can (1/ ^{o}C)
	AUSSRA	linear radial expansion coefficient for structure material (1/ ^{o}C)
	AUSKUE	volumetric expansion coefficient for coolant (1/ ^{o}C)
K9	KKN	number of the segment
	MDD	Number of different Doppler data sets, i.e. different initial compositions in the segment
	((BEZUGT (I,J), XF(I,J), XC(I,J), AFSIG(I,J) AFSIGC(I,J), I=1,NG) J=1,MDD)	here the punched output of DOPKIN for the compositions in the radial segment is to be inserted

	(MZD(I), I=1,NM)	each axial zone is assigned one of the Doppler data sets according to the value of MZD

S10 if KØNSI=0 (see card K21 of basic KINTIC-1 input), end of thermodynamics input, otherwise proceed with S11

S11 for each radial segment K12

K12	KKN	number of the segment
	NTT	number of following temperature sets
	(TFIN (I),	initial fuel temperature as used in NUSYS for the calculation of the cross sections /$^{-o}$C/
	TCIN(I)	initial can temperature /$^{-o}$C/
	TKIN (I),	initial coolant temperature /$^{-o}$C/
	TSIN (I), I=1,NTT)	initial structure material temperature /$^{-o}$C/
	(MI (I), I=1, NM)	each axial zone is assigned one of the above initial temperature sets according to the value of MT

S13 end of thermodynamics input

For the DIXY input, the format is given in addition to card number, variable name and explanation. Otherwise, the rules for presenting the input list are unchanged.

DIXY input

K1	A4	DIXY	constant

S2 case identification with K9 and K4, otherwise go to K5

K3	A4, I4	NØTE	constant

		NK4	number of K4 type cards
K4	A80		Column 2 - 80 make up the case identification. Attention: Column 1 is used as carriage control
K5	A4, I4	KN	constant
		NKN	$\leq$18, number of variables in K6; final data with value 0 may be omitted
K6	18I4	IGEØ	geometry index (1=XY, 2=RZ, 3=R-Theta)
		M	number of mesh rows ($\leq$148, multiple of 4)
		N	number of mesh columns($\leq$148, multiple of 2)
		NGP	number of energy groups
		NM	number of compositions
		IZØ	number of regions ($\leq$100, NM $\geq$ IZØ)
		0	constant
		0	constant
		IQUE	0 internal DIXY-estimate of source distribution 4 as initial estimate the source of a preceding diffusion calculation is expected on file NFZ1
		0	constant
		1	constant
		ITMAX	maximum number of source iterations
		NFZ1	data set reference number ($1 \leq NFZ1 \leq 99$; NFZ1 $\neq$ 5,6,7,13,20,21,22) for internal file
		JØINT	0 if KØNSI $\neq$ 1 and KØNE $\neq$ 1 1 otherwise
		0	constant
		IDIT	5 no DIXY printout of flux and source 0 source distribution is printed 1 source and flux distribution is printed

Since the DIXY flux is not normalized in accordance with eq.(6) from part 1 of this report, flux printout is better effected by using IDIT=0 and NAUS=1 (basic KINTIC-1 input)

		KRI	0 no radius iteration 1,2,3 to reach k_{eff}=XKEND (K8), region NRRI is initially extended horizontally (1), vertically (2), or both (3) -1,-2,-3 same as above, but region NRRI is initially contracted
		NRRI	number of a corresponding K11 card, if KRI≠0; otherwise NRRI=0
K7	A4,I4	CN	constant
		NCN	number of variables in K8
K8	10E8.5	EPK	relative accuracy of k_{eff} and source
		EPF	relative accuracy of fluxes
		CTØP	top boundary constant
		CRGHT	right boundary constant
		CBTTM	bottom boundary constant
		CLEFT	left boundary constant the boundary constants may have the following values: 0. for flux=0 $\geqslant 10^8$ for current=0 $0 \leqslant C < 10^8$ for extrapolated flux=0 with $3 \cdot C \cdot D_g$ as extrapolation distance
if KRI > 0, continue with ENDK and EPS, otherwise end of card			
		ENDK	desired k_{eff} value
		EPS	accuracy for ENDK
K9	A4	REGN	constant

S10 for each zone a card K11. The order of zones is given by the prescriptions at the beginning of this chapter. Each zone must contain at least one mesh point which is not situated on a boundary. Indexing goes vertically from top to bottom, horizontally from left to right.

K11	5I4	MIN	composition number
		IL	left region boundary index
		IR	right region boundary index
		JT	top region boundary index
		JB	bottom region boundary index
K12	A4	HSTP	constant
K13	6(I4,E8.5)	NK13	number of data in K13 without NK13 ($\leqslant 150$)
		HO	left reactor boundary, generally O. /cm/
		N1	number of uniform steps from HO to H1
		H1	next abscissa with step change /cm/
		N2	similar to N1
		H2	similar to H1
		.	
		.	
		HN	right reactor boundary
K14	A4	VSTP	constant
K15	6(I4,E8.5)	NK15	number of data in K15 without NK15 ($\leqslant 148$)
		VO	coordinate of the top reactor boundary /cm/
		M1	number of uniform steps from VO to V1
		V1	next coordinate with step change /cm/
		M2	similar to M1
		V2	similar to V1
		.	
		.	
		VM	bottom boundary coordinate, normally O.

S16 if relaxation parameter input exists, continue with K17 and K18, otherwise branch to S19

K17	A4	OMEG	constant
K18	10E8.5	(O(L), L=1,NGP)	list of omega parameters

S19 if a source guess is to be built up by 1d axial and radial distributions, continue with K20-K22, otherwise S23

K20	A4	S1X1	constant
K21	10E8.5	(QH(L), L=1,N)	list of radial (horizontal) source
K22	10E8.5	(QV(L), L=1,M)	list of axial (vertical) source

S23 for a 2d source guess continue with K24-K26, otherwise K27

K24	A4	S2X1	constant

S25 for each mesh row with index J, J=1, M : K26

K26	10E8.5	(QJ(L), L=1,N)	source vector for J'th mesh row
K27	A4	DXNF	constant
K28	A4,I4	SIGM	constant
		20	constant, ds.-ref. for KINTIC-1 cross section file

S29 for buckling input continue with K30-S34, otherwise K35

K30	A4,I4	BUCK	constant
		IBUCK	1 uniform buckling
			2 composition dependent buckling
			3 group dependent buckling
			4 group and composition dependent buckling

S31 if IBUCK=4, for each group a pair K32, K33, otherwise only one such pair

K32	I4	MX	1 for IBUCK=1
			NM for IBUCK=2 or 4
			NGP for IBUCK=3
K33	6E13.6	(B2(L), L=1,MX)	bucklings $/cm^{-2}/$

S34 continue with K36

K35	A4	BLNK	constant
K36	A4	DXND	constant, end of input

As implied in the cards S15-K19 in the basic KINTIC-1 input, a restart option is built into KINTIC-1. Instead of calculating until the end of the specified perturbation intervals, one may stop after a prescribed number of macro intervals, save all significant data on files and restart the calculation in a seperate run. This may be done several times. One useful application of this option is for checking the input data by using NCHEC=1 or 2, in which case only the steady state calculations with or without temperature distributions are done.

After verifying the correctness of the results, one may continue with the transient calculations.

Normally, only the direct access file must be reserved for the restart. In this case, two restart possibilities are available:

1. Before continuing, the direct access file is copied to another direct access file with data set reference number 23. If the restart job fails, e.g. due to a machine error, it may be repeated with the duplicate file.

2. The direct access file is not copied. If, in this case, a machine error occurs, the calculation must be repeated from the beginning.

For very big cases, the space available on the direct access data set may not suffice to accommodate the data necessary for the restart. In this case, one or two additional files must be reserved. Their numbers are printed at the end of the job. KINTIC-1 provides only the restart option 2 - without data set copy - for these cases.

The input for a restart run is given below. It is unformatted.

Input for restart

K1	ϑCHECKIϑ	constant
K2	NCHECI	value of NCHEC from foregoing run
	NSATZ	the constant printed at the end of the foregoing run (a message: "restart possible with NSATZ = ... " is printed for each check point). If this constant is made negative, the direct access data set is copied before the calculation continues, otherwise this is not done.

K3 KTPØUT >0 data set reference number for storage of tape output, if new tape is to be used for continuation job.
$=0$ no tape output
<0: - KTPØUT = data set reference number of tape containing the results of foregoing job.

XLABEL 16 alphanumerical characters as label for the DYNEVA data file; must equal XLABEL from foregoing job if KTPØUT <0

S4 if the calculation is to proceed to its end K5, otherwise K7

K5 ∂ENDE∂ constant

S6 end of input

K7 ∂CHECK∂ constant

K8 NCHEC, MAKMAX } see K19 of basic KINTIC-1 input; if NCHECI=1 or 2, NCHEC $>$NCHECI

S9 end of input.

The control cards for KINTIC-1 are given next after some remarks on the internal organization of the code.
Adjustable dimensioning has been used, i.e. the storage requirement is a function of the case to be calculated. Typically, a main storage region of 300 K bytes is sufficient for a 6 energy group, 6 precursor group, 46 composition, 1450 mesh point case (SEFOR). For smaller cases 240 K, or for test cases 180 K, suffice.

The program internally checks the amount of storage provided and prints one of the following messages:

1. The amount by which the REGION-parameter may be reduced, if the storage is bigger than needed.

2. A message saying that the storage is adequate.

3. A warning, if the storage fits the case very closely.

4. The amount by which the REGION-parameter must be enlarged, if the storage is too small.

In the last case, the calculation is terminated after output of the message.

Four, or in the case of a DYNEVA evaluation tape being produced, five data sets are used. They are

1. The internal data set given in card K6 of the DIXY input (NFZ1). It is used for storing the DIXY-results.

2. The data set 20, containing the KINTIC-1 cross sections produced by NUSYS. Internally, it is used for storing the cross sections in the format needed by DIXY and the inhomogeneous source for shape function recalculation. The initial contents of this data set is destroyed. Therefore, before starting KINTIC-1, the original NUSYS-data set is copied and KINTIC-1 works with this copy.

3. A direct access data file with the data set reference number 21, containing 300 2200 byte records (i.e. for this file, SPACE=(2200,(300)))

4. A segmential file with data set reference number 22 used for storage of intermediate data.

5. For creation of an evaluation tape for DYNEVA, a reserved tape has to be specified in addition to the four previous files.

In case of a restart job, the first four data sets specified above must be reserved for use with the follow-up job. Of course, the evaluation tape is reserved, as well. Three possibilities exist for the evaluation tape of the follow-up job: The evaluation tape of the preceding job may be continued, a new evaluation tape may be started, or no evaluation tape may be used. Likewise, a follow-up job may start with a new evaluation tape, if none has been created by the preceding job.

During processing of the input data, a rewind is made for rading the data again. With the ASP-operating system, this cannot be done, if the input cards are inserted in the KINTIC-1 step with the usual G.SYSIN control card. Instead, the input file has to be created before using the procedure EBCDIC. If the internal KINTIC-1 data sets are to be reserved for later runs, this jobstep, as well, may be used for deleting possibly existing reserved data sets with the same name.

The KINTIC-1 job therefore, normally has five jobsteps:

1. Procedure EBCDIC for deleting duplicate data sets and creating the input file.

2.-4. Utility programs for duplicating the NUSYS-data files.

5. The KINTIC-1 jobstep.

A continuation job consists only of the KINTIC-1 jobstep. For a test case using a simple cross section input, which is created in a foregoing NUSYS step in the same job, the jobsteps 2-4 may be deleted.

A list of control cards for a job involving a reactor with 46 compositions, 6 energy and precursor groups, 1450 mesh points and three coolant channels with 6 axial segments (case cited above and in chapter III) is presented below. The cross section data set has the name dsname and is in the library dkname; its duplicate is to be brought into the library dlname. Furthermore, KTPØUT=19 and NFZ=10 are assumed. The job is run with NCHEC=2, i.e. the five data sets will be reserved and later used in a continuation run. It is assumed that the data sets with data set reference number 10, 21 and 22 have the names dsn0, dsn1 and dsn2 and are stored in the library dkname.The tape is assumed to be a DV-tape with number nnnn and is given the name dsnt (in Karlsruhe, the so-called "DV"-tapes are kept in the machine room; they are automatically mounted if requested by the DD-card of a job.).

List of control cards for initial job

```
//usual job card with REGION=300K
/*SETUP DEVICE=TAPE9,ID=DVnnnn
// EXEC EBCDIC,PARM.S=NØCØ
//S.FT04F001 DD DSN=&KINTIN,UNIT=DISK,DISP=(NEW,PASS),
// SPACE=(TRK,8)
//S.FT10F001 DD DSN=dsn0,UNIT=2314,VØL=SER=dkname,
// DISP=(ØLD,DELETE)
//S.FT11F001 DD DSN=dsn1,UNIT=2314,VØL=SER=dkname,
// DISP=(ØLD,DELETE)
//S.FT12F001 DD DSN=dsn2,UNIT=2314,VØL=SER=dkname,
// DISP=(ØLD,DELETE)
//S.SYSIN DD *
    Total KINTIC-1 input
// EXEC PGM=IEHPRØGM
//SYSPRINT DD SYSØUT=A
```

```
//A1 DD DSN=dsname,UNIT=2314,VØL=SER=dlname,
// DISP=(ØLD,DELETE)
//SYSIN DD DUMMY
// EXEC PGM=IEHPRØGM
//SYSPRINT DD SYSØUT=A
//DN1 DD DSN=dsname,UNIT=2314,VØL=SER=dlname,
// DISP=(NEW,KEEP),SPACE=(TRK,25)
//SYSIN DD DUMMY
// EXEC PGM=IEHMØVE
//SYSPRINT DD SYSØUT=A
//SYSUT1 DD UNIT=DISK,SPACE=(TRK,100)
//DA1 DD UNIT=2314,VØL=SER=dlname,DISP=ØLD
//DA2 DD UNIT-2314,VØL=SER=dkname,DISP=ØLD
//SYSIN DD *,DCB=BLKSIZE=80
  CØPY DSNAME=dsname,FRØM=2314=dkname,TØ=2314=dlname
// EXEC FHG,LIB=NUSYS,NAME=KINTIC,REGION.G=300K
//G.FT05F001 DD DSN= &KINTIN,DISP=(ØLD,DELETE)
//G.FT08F001 DD UNIT=DISK,SPACE=(TRK,8)
//G.FT10F001 DD DSN=dsn0,UNIT=2314,VØL=SER=dkname,
//  DISP=(NEW,KEEP),SPACE=(TRK,15)
//G.FT19F001 DD UNIT=TAPE9, VØL=SER=DVnnnn,
// DSN=dsnt,DISP=(,PASS), DCB=(BLKSIZE=1016,RECFM=VS)
//G.FT20F001 DD DSN-dsname,UNIT=2314, VØL=SER=dlname
// DISP=(ØLD,KEEP)
//G.FT21F001 DD DSN=dsn1,UNIT=2314,VØL=SER=dkname,
// DISP=(NEW,KEEP), SPACE=(2200,(300))
//G.FT22F001 DD DSN=dsn2,UNIT=2314,VØL=SER=dkname,
// DISP=(NEW,KEEP),SPACE=(TRK,5)
//   "end of job" card                                          //
```

Next, a list of the control cards for the continuation job of the above job is given. It is assumed that the calculation time for this job has been estimated as 70 minutes. In this case, i.e. if the time for one jobstep is more than 60 minutes, it must be given in the exec-card of the step as

well als in the jobcard. Furthermore, NSATZ is assumed to be negative and the data set used for the copy of the direct access data set is given the name dsn3.

List of control cards for continuation job

```
// usual job card with REGIØN=300K,TIME=70
//SETUP  DEVICE=TAPE9,ID=DVnnnn
// EXEC FHG,LIB=NUSYS,NAME=KINTIC,REGIØN.G=300K
// TIME.G=70
//G.FT08F001 DD UNIT=DISK,SPACE=(TRK,1)
//G.FT10F001 DD DSN=dsn0,UNIT=2314, VØL=SER=dkname,
// DISP=(ØLD,DELETE)
//G.FT19F001 DD UNIT=TAPE9,VØL=SER=DVnnnn,
// DSN=dsnt,DISP=(,PASS),DCB=(BLKSIZE=1016,RECFM=VS)
//G.FT20F001 DD DSN=dsname,UNIT=2314,VØL=SER=dlname,
// DISP=(ØLD,DELETE)
//G.FT21F001 DD DSN=dsn1,UNIT=2314,VØL=SER=dkname,
// DISP=(ØLD,DELETE)
//G.FT22FT001 DD DSN=dsn2,UNIT=2314, VØL=SER=dkname
// DISP=(ØLD,DELETE)
//G.FT23F001 DD DSN=dsn3,UNIT=2314,VØL=SER=dkname,
// DISP=(NEW,KEEP),SPACE=(2200,(300))
// "end of job" card
```

At the end of this chapter, some remarks should be made on the different levels of printed output. The output of diffusion calculation results is governed by IDIT (Dixy input, card K6). As explained there, one should not use IDIT=1, if one is interested in the flux distribution, but rather NAUS= -1. With any value of IDIT, some intermediate results of each outer iteration for a diffusion calculation are printed, especially k_{eff}, which may enable the user to gather some information on the convergence of his problem.

Apart from the DIXY output, the whole output is directed by NAUS (basic KINTIC-1 input, card K3). The lowest level of output, i.e. NAUS=0 gives the following output lists in addition to the usual DIXY output comprising initial geometry information and the data governed by IDIT: A list of the unformatted input; zone dependent power distribution and total power; initial temperature distribution in fuel, can, coolant and structure material; flux amplitude as a function of micro steps; reactivity, lifetime and β_{eff}^{i} as a function of normal steps; for each normal step, the axial temperature distribution at the fuel centre and in the coolant; and some messages concerning the flow of the calculation, e.g. number of normal step (inner) iterations and recalculation of a macro step. With NAUS= -1, one gets in addition: The normalized shape function; the total temperature distribution, and the altered dimensions of the reactor zones. With NAUS= -2 zone dependent β^{i} and λ^{i} and some other values are printed in addition. NAUS=1 is an option for testing purposes and should be used only if numerical difficulties are encountered or if the user looks for a way of producing tons of paper. The normal procedure would be to use KINTIC-1 with a minimum printed output (NAUS=0 or = -1), determining the areas of interest from this. Then, DYNEVA would be used to produce plots from the evaluation tape.

V. Input for sample case

As an example for a calculation with KINTIC-1 the input and control cards for the MITKIN test case 6 given in part 1 of this report will be listed. The results may be taken from this report ($\Delta\sigma_c$ = - .009). The job involves no thermodynamics and feedback, and the NUSYS and KINTIC-1 jobsteps are integrated in one job.

Job control cards:

```
// usual job card with REGIØN=240K,TIME=3
// EXEC FHG,LIB=NUSYS,NAME=ANUSY,PARM.G=90000
//G.FT02F001 DD UNIT=DISK,SPACE=(TRK,8)
//G.FT20F001 DD DSN= &CRØSEC,UNIT=DISK,DISP=(NEW,PASS),
// SPACE=(TRK,10)
//G.SYSIN DD *
     NUSYS input cards
// EXEC EBCDIC,PARM.S=NØCØ
//S.FT04F001 DD DSN= &KINTIN,UNIT=DISK,DISP=(NEW,PASS),
// SPACE=(TRK,8)
//S.SYSIN DD *
     KINTIC-1 input cards
// EXEC FHG,LIB=NUSYS,NAME=KINTIC
//G.FT05F001 DD DSN= &KINTIN,DISP=(ØLD,DELETE)
//G.FT08F001 DD UNIT=DISK,SPACE=(TRK,8)
//G.FT10F001 DD UNIT=DISK,SPACE=(TRK,15)
//G.FT20F001 DD DSN= &CRØSEC,DISP=(ØLD,DELETE)
//G.FT21F001 DD UNIT=DISK,SPACE=(2200,(300))
//G.FT22F001 DD UNIT=DISK,SPACE=(TRK,5)
//    "end of job" card                                    //
```

Since this job has a card input of cross sections, the data set references 4 and 15 from the example of job control cards for the NUSYS step are deleted.

Furthermore, no data sets have to be kept after completion of the job and therefore none is brought into a library.

Next the NUSYS input is given. It consists of the input for the module sequence 397/451/2250 according to the first example for the NUSYS module queuing cited in chapter III.

```
$00397$
451 0  0  0
$ENDE$
$00451$
2250 0  1  0
$SPEC$
0  $SABBR$
2  2  3
8  $CHI$  0  $ $ 1  1.   0
8  $CHI$  0  $ $ 2  1.   0
8  $CHI$  0  $ $ 3  1.   0
8  $NUSF$   0 $M$   1    .00765695      .21877
8  $NUSF$   0 $M$   2    .00765695      .21877
8  $NUSF$   0 $M$   3    .00328155      .065631
8  $SCAPT$ 0 $M$     1    .0065  .05
8  $SCAPT$  0 $M$    2    .0065  .041
8  $SCAPT$  0 $M$    3    .0065  .02
8  $SFISS$  0 $M$    1    .0035  .1
8  $SFISS$  0 $M$    2    .0035  .1
8  $SFISS$  0 $M$    3    .0015  .03
8  $SMIØT$  1 $M$    1    0   0
8  $SMIØT$  1 $M$    2    0   0
8  $SMIØT$  1 $M$    3    0   0
8  $SMIØT$  2 $M$    1    .01      0
8  $SMIØT$  2 $M$    2    .01      0
8  $SMIØT$  2 $M$    3    .01      0
```

```
8   'SREM'    0   'M'    1     .02      .15
8   'SREM'    0   'M'    2     .02      .141
8   'SREM'    0   'M'    3     .018     .05
8   'STR'     0   'M'    1   .2380952    .8333333
8   'STR'     0   'M'    2   .2380952    .8333333
8   'STR'     0   'M'    3   .2564103    .6666667
8   '1/V'     0   ' '    1     1.E-7      5.E-6
8   '1/V'     0   ' '    2     1.E-7      5.E-6
8   '1/V'     0   ' '    3     1.E-7      5.E-6
0   'KØMPØ'
11  'XXXXXXXXXXX' 0  2  3  0  1
2  'M'
3  1  1  1.
3  1  1  1.
3  1  1  1.
0  'ENDE'
'NØRM'
 '02250'
2290   2   3   2
1   4   5   3   6   7
1   1
1.  0
'M'   .0075    .08
1
'BRENN'  1    M    1.
1
'BRENN'  1    M    1.
1
'BRENN'  1    M    1.
1
1    2
'NUFIN'
```

One can deduce from this input that three compositions are defined; two of them make up the reactor, the other one (composition 2) is only used for defining the perturbation. The duplicate compositions 3 and 4 equal composition 1, 6 and 7 equal composition 3. Since no feedback is used, only one macro material is defined, consisting of the pseudo-isotope M. One precursor group with β =.0075 and λ = .08 and delayed spectrum = prompt spectrum is employed.

The KINTIC-1 input is as follows:

```
$START$
2  1  6  576  0  0  0
-1  0 '                    '
$PERTUR$
1
4  .2  1  1  1
$CØNTRØL$
0  0  1.  0
1.-5  1.-4  .005  .00001  .02  .02  .002  .1  .1
$PØWER$
1.
$ØMEGA$
1.  1.  1.  1.  1.  1.
$ENDE$
$CØNSIS$
0  0  0
$FEEDBACK$
0 0 0 0 0 0 0 0 1
$FØRM$
```

The formatted part of the input directly following these cards will be given on the next page.

```
DIXY
NØTE   1
 MITKIN TEST CASE 6
KN    16
   1  24  24   2   7   6   0   0   0   0   1  30  10   1   0   5
CN     6
    .001    .001       0       0 1.E+10 1.E+10
REGN
   6   1  18   1   7
   7  18  24   1  24
   4   1   7   7  18
   3   1   7  18  24
   1   7  18   7  18
   5   7  18  18  24
HSTP
  11      0.   4    20.   4    28.   7    52.   4    60.   4    80.
VSTP
  11     80.   4    60.   4    52.   7    28.   4    20.   4     0.
DXNF
SIGM  20
BLNK
DXND
```

VI. Internal structure of KINTIC-1

It is not possible in the framework of this report to give the FORTRAN listing of KINTIC-1, since it comprises about 5000 cards. Such listing may be made available by the authors. Instead, some information on the internal structure of KINTIC-1 is presented here. It is not necessary for the user to read this chapter, but it may be quite useful for gathering some understanding of the organization and the flow of calculations.

The program has a modular structure with a main program governing the flow of calculations. The data are arranged in blocks which are stored in a central file (the direct access file 21). A few fundamental data are in common. Furthermore, there is a data field available to all modules, whose length is determined from the region-parameter and the storage needed for the program itself. Each module reads its specific data blocks into this field, stores intermediate data there and, before giving control back to the main program, stores altered or new blocks back into the central file. Furthermore, small additional data files had to be used as communication with already existing codes, mainly DIXY. Details of the calculations done by KINTIC-1 and the interaction of the modules are given in the first part of this report. A survey of the whole program may be gathered from figures 16 and 17, which give the flow charts of the steady state and dynamic calculations. Some variable names have been used in these charts, whose meanings are:

NCHECI	= Checkpoint number of foregoing job
NCHEC	= Checkpoint value of current job
ITER	= Current number of macro step iterations
ITERMX	= Maximum number of macro step iterations
T	= current time
TST2	= end of current perturbation interval
TMAX	= maximum value for end of normal interval
TMAKRØ	= maximum value for end of macro interval
ER4	= value determining the new shape function calculation

A few hints should be given for a better understanding of the two flow charts. The same program part, that of fig. 16/2 is used for determining consistent cross sections and for carrying out the k_{eff}-search. This part is not reached if DIXY is used for a k_{eff}-search. In fig. 17, the intricate combinations of logical decisions have but one aim, namely to decide after a normal step has been successfully iterated, whether a new shape function is to be calculated, because either the end of a perturbation interval is reached or the shape function has become inadequate; if this is not the case, one must decide whether one has just reached the point at which a new shape function is to be employed.

VII. Conclusion

This report is intended to serve a twofold purpose: To give a compilation of the physical models making up the current version of the two-dimensional quasistatic code with feedback, KINTIC-1, and to present a code description enabling a prospective user to run the program. A description of the evaluation program DYNEVA will be issued shortly. Supplementary descriptions of future versions of KINTIC are planned.

First calculations with KINTIC-1 have proven the code to be an accurate and useful tool for calculating the initial stages of an excursion or experimental transients like the SEFØR experiments. It is a very convenient tool as well due to its elaborate time step automatization. With the inclusion of additional modules, future versions of KINTIC will be able to treat the processes characteristic of more serious and realistic excursions.

Literature:

1. G. Kessler: Space-Dependent Dynamic Behavior of Fast Reactors Using the Time-Discontinuous Synthesis Method, Nucl. Sci. Eng. 41, 115 (1970)

2. D.A. Meneley et al.: A Kinetics Model for Fast Reactor Analysis in Two Dimensions. Presented at the Symposium on Dynamics of Nuclear Systems, Tucson, Arizona, March 23-25, 1970

3. K.O. Ott: QX2S, private communication

4. E. Vincenti, A. Clusaz: Constanza (R,Z), EUR-4673, 1971

5. D. Babala et al.: Andycap - A Three-Dimensional Computer Programme for Transient Analysis of Boiling Water Reactors. Reaktortagung Bonn, 30.3. - 2.4.1971. Tagungsbericht, p. 238

6. K.O. Ott, D.A. Meneley: Accuracy of the Quasistatic Treatment of Spatial Reactor Kinetics. Nucl. Sci. Eng. 36, 402 (1969)

7. L.P. Abagjan et al.: Gruppenkonstanten schneller und intermediärer Neutronen für die Berechnung von Kernreaktoren. KFK-tr-144

8. R. Froelich: Theorie der Dopplerkoeffizienten schneller Reaktoren unter Berücksichtigung der gegenseitigen Abschirmung der Resonanzen KFK 367, 1965

9. I. Siep: Zur Berechnung von Dopplerkoeffizienten für schnelle Reaktoren. KFK 983, 1969

10. W. Höbel: to be published and abstract No. ENEA 184 of the ENEA Computer Programme Library

11. D.A. Meneley et al.: Space-Time Kinetics - The QX1 Code ANL 7310

12. A.F. Henry: The Application of Reactor Kinetics to the Analysis of Experiments. Nucl. Sci. Eng. 3, 52 (1958)

13. E.G. Schlechtendahl: Sieden des Kühlmittels in natriumgekühlten schnellen Reaktoren. KFK 1020, 1969.

14. L.R. Blue, M. Hoffman: AIREK3; Generalized Program for the Numerical Solution of Space Independent Reactor Kinetics Equations. AMTD-131, 1963

15. R. Froelich, S.R. Johnson: Exact Solution of the Non-Linear Prompt Kinetics Equations. A Benchmark Problem in Reactor Kinetics. Nukleonik 12, 93 (1969)

16. G. Buckel: Approximation der stationären drei-dimensionalen Mehrgruppen-Neutronen-Diffusionsgleichung durch ein Syntheseverfahren mit dem Karlsruhe Synthese-Programm KASY. KFK 1349 (1971)

17. W.H. Reed, K.F. Hansen: Finite Difference Techniques for the Solution of the Reactor Kinetics Equations. MIT-3903-2, 1969

18. J.B. Yasinsky: Numerical Studies of Combined Space-Time Synthesis. Nucl.Sci.Eng. 34, 158 (1969)

19. J.B. Yasinsky, M. Natelson, L.A. Hagemann: TWIGL-A Program to Solve the Two-Dimensional, Two-Group, Space-Time Neutron Diffusion Equations with Temperature Feedback; WAPD-TM-743(1968)

20. D. Wintzer, private communication

21. E. Kiefhaber: The KFKINR-Set of Group Constants; Nuclear Data Basis and First Results of its Application to the Recalculation of Fast Zero-Power Reactors; KFK 1572 (1972)

22. D. Gorenflo, D. Sanitz et al.: unpublished

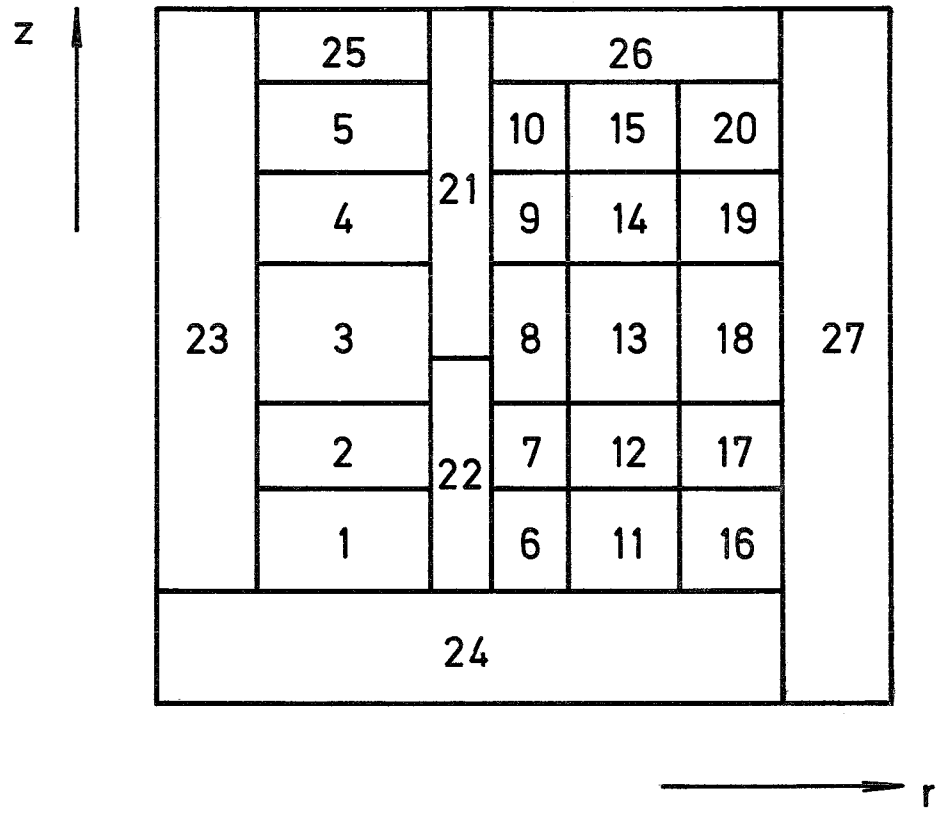

Fig.1: Example for the geometrical representation of a cylindrical reactor with feedback

Zones	1-5	1.radial segment
	6-10	2.radial segment
	11-15	3.radial segment
	16-20	4.radial segment
	2-4	Inner core
	7-9,12-14	Outer core
	16-20	Radial blanket
	1,6,11	Lower axial blanket
	5,10,15	Upper axial blanket
	21,22	Partially inserted control rod
	23	Central loop
	24	Lower axial reflector
	25,26	Upper axial reflector
	27	Radial reflector

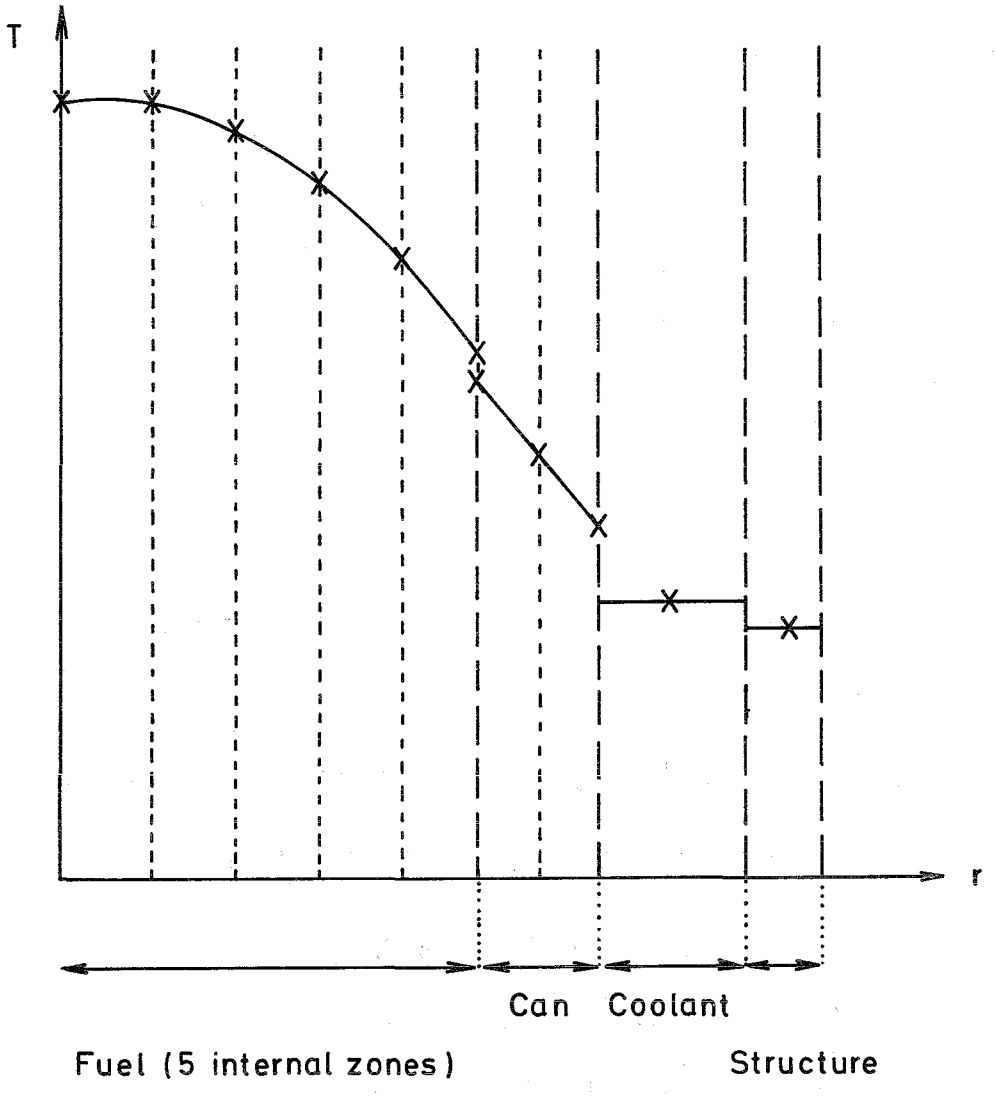

Fig. 2 · Geometrical representation of the coolant channel with fictitious temperature distribution.

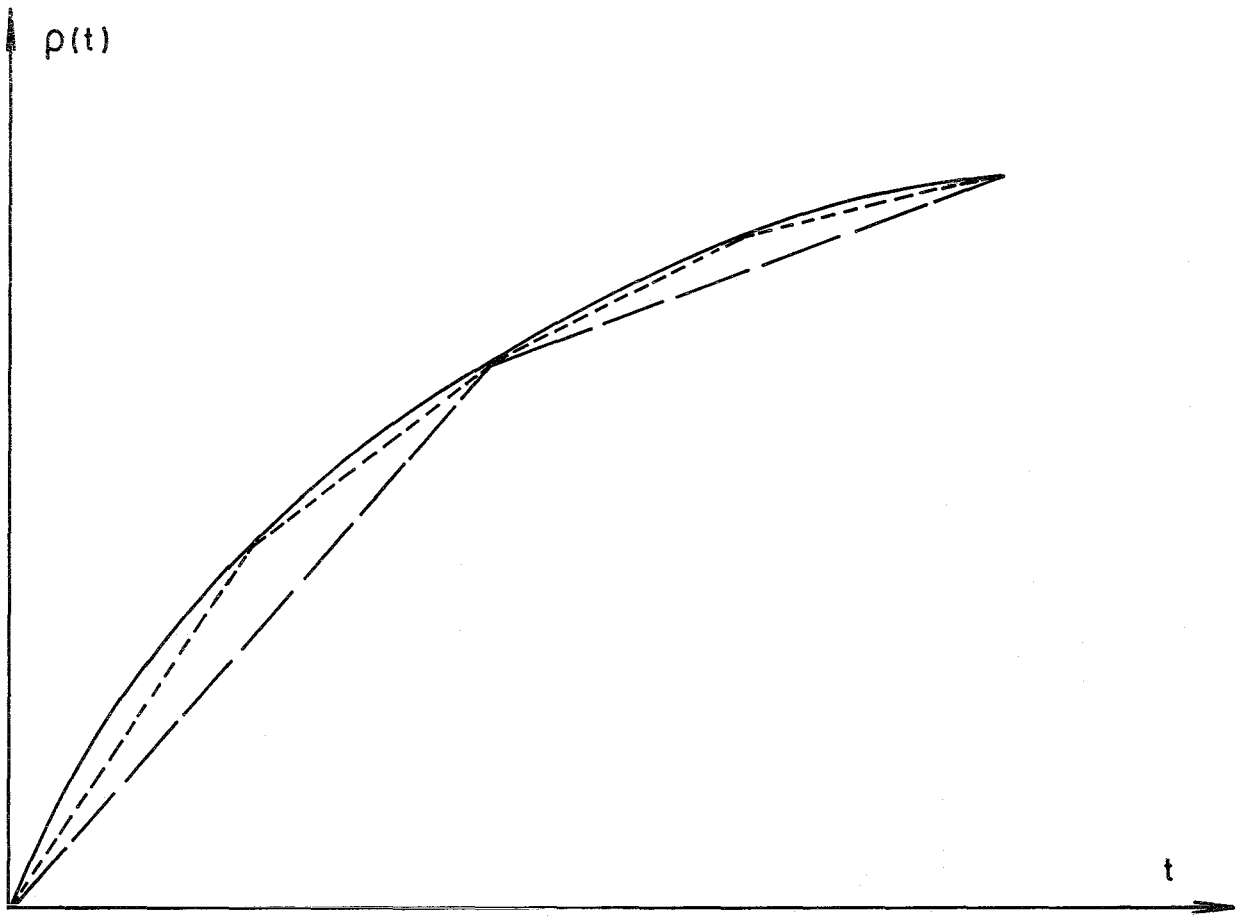

Fig.3: Error introduced by zonal treatment of perturbation event.

——— true reactivity

— — approximation for two perturbation zones

----- approximation for four perturbation zones

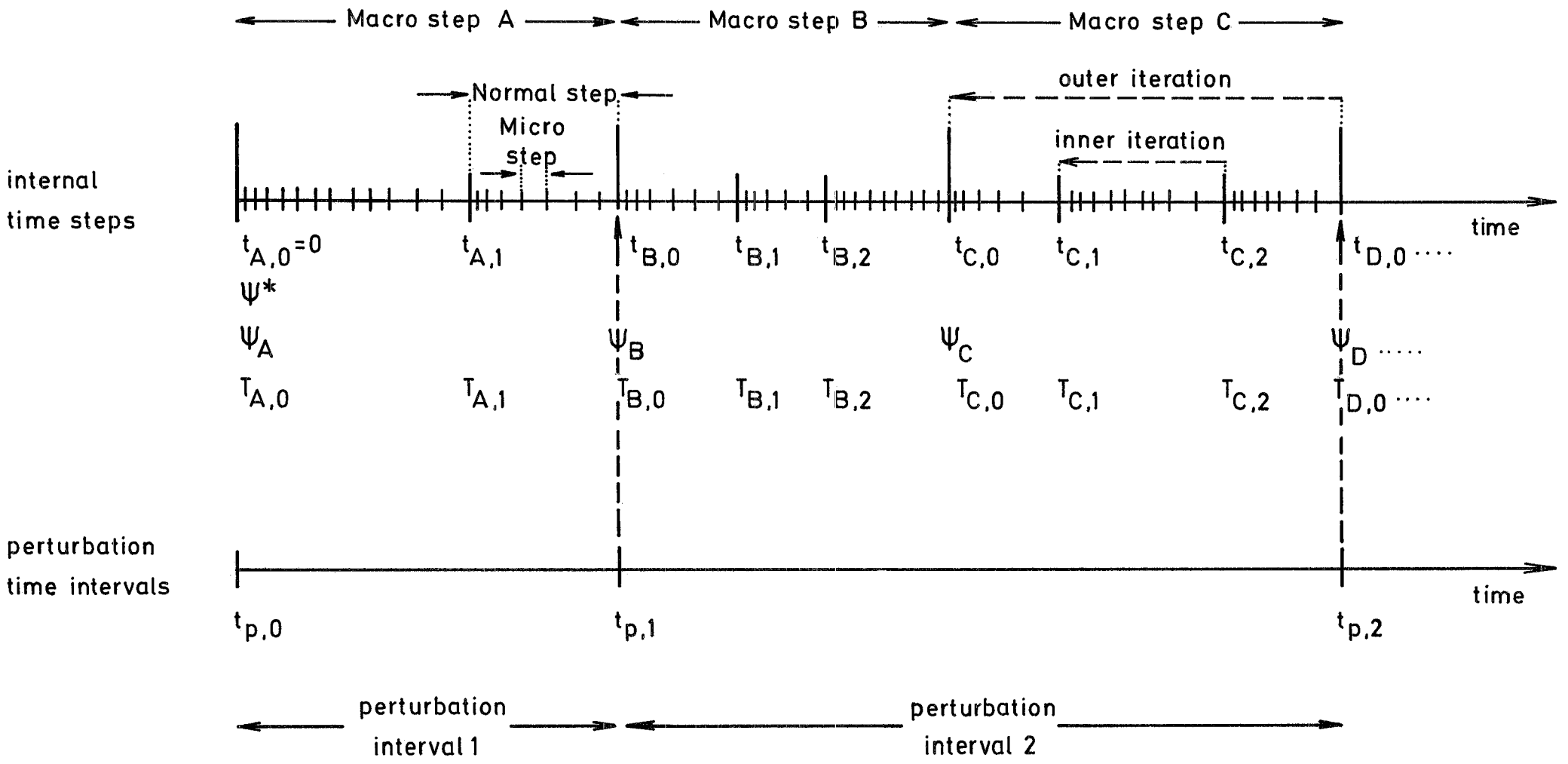

Fig. 4: Example for time scale division in quasistatic calculations.

t : time; Ψ: shape function; T: temperature distribution.

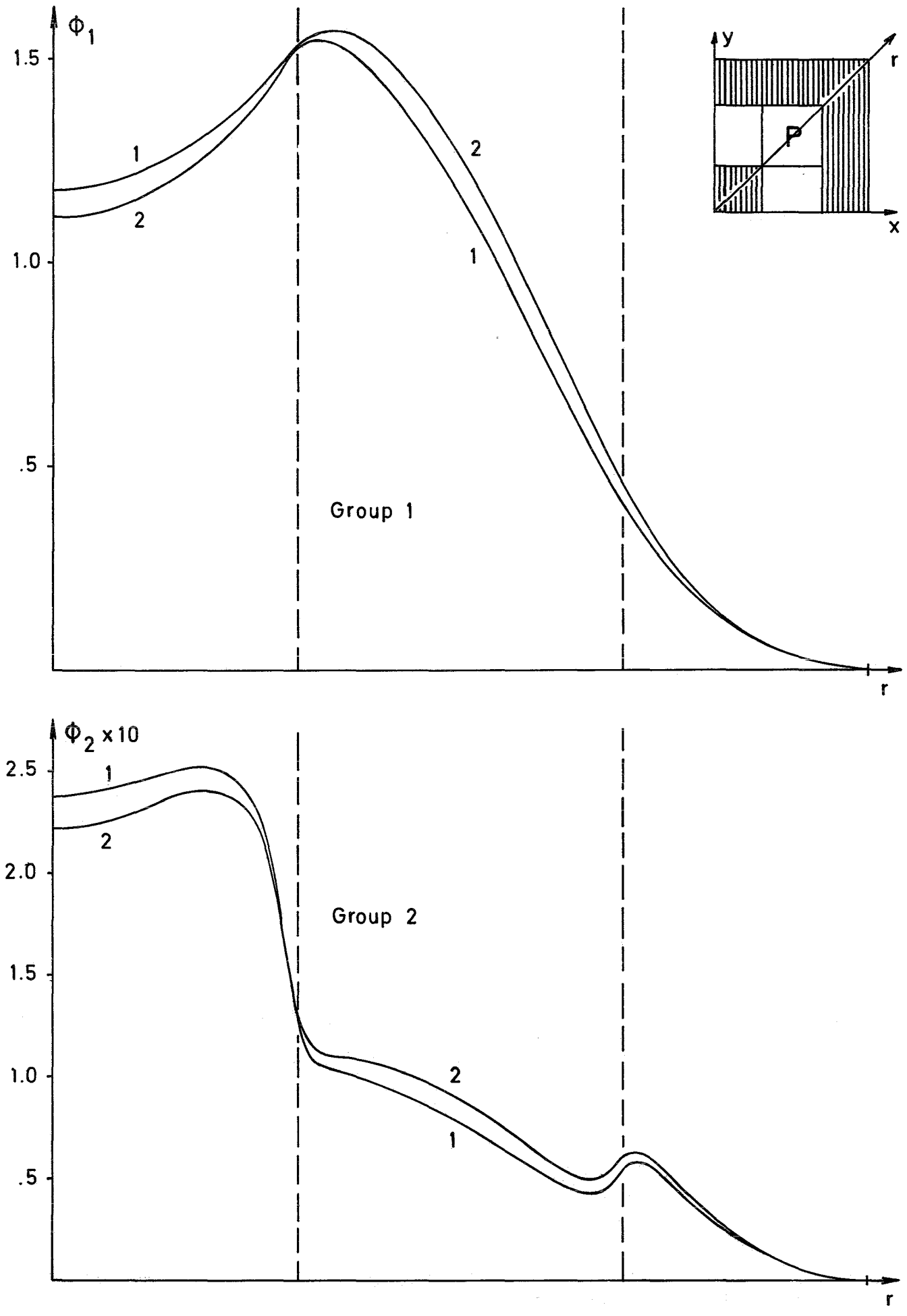

Fig. 5: Flux distribution for MITKIN test case 6

1 steady state ; 2 end of ramp with $\Delta\sigma_c = -.009$

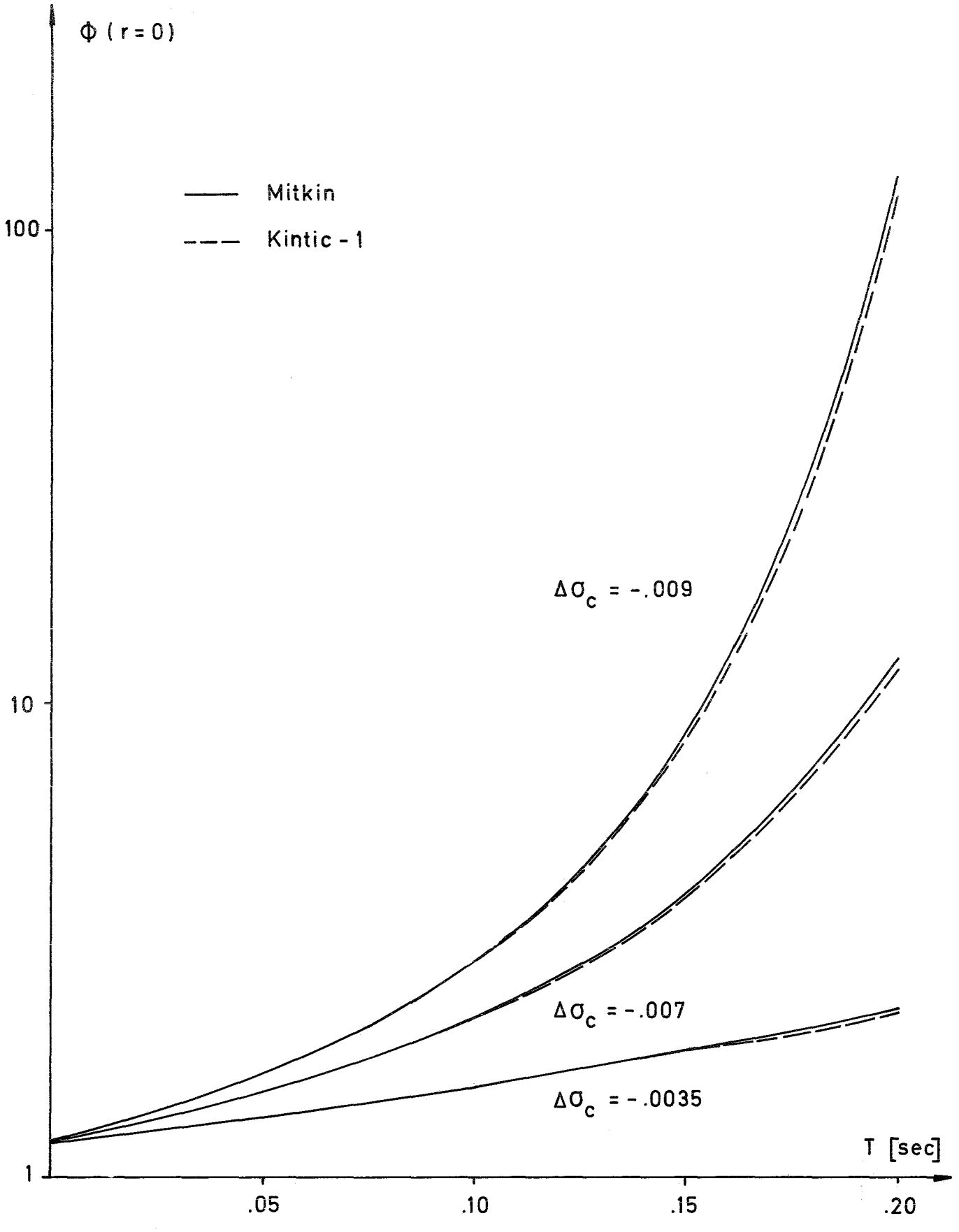

Fig. 6: Time dependent fast flux in reactor centre for MITKIN test case 6

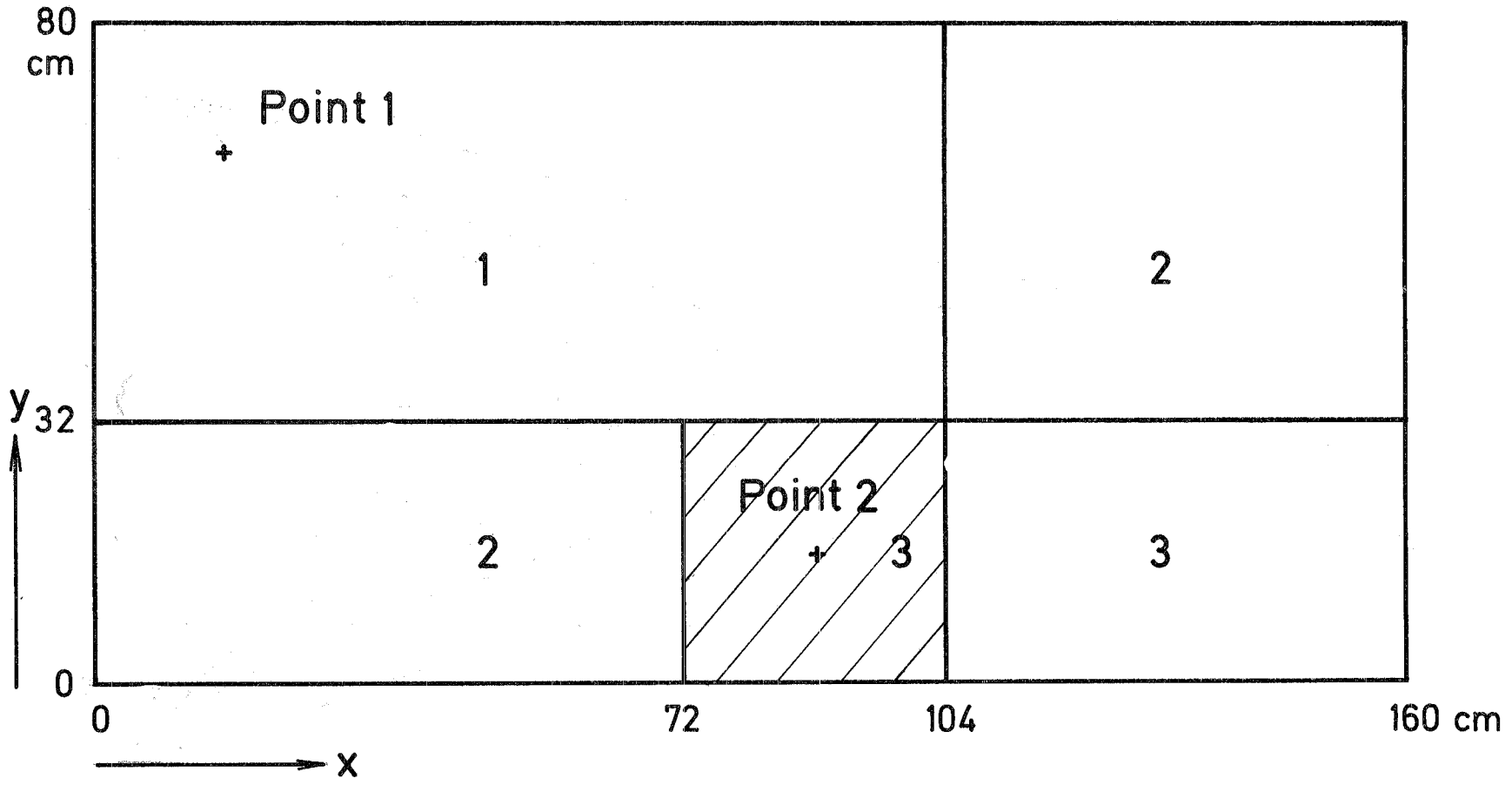

Fig. 7 : Geometry for MITKIN test case 8 . Numbers indicate different compositions. Perturbation induced in cross-hatched region.

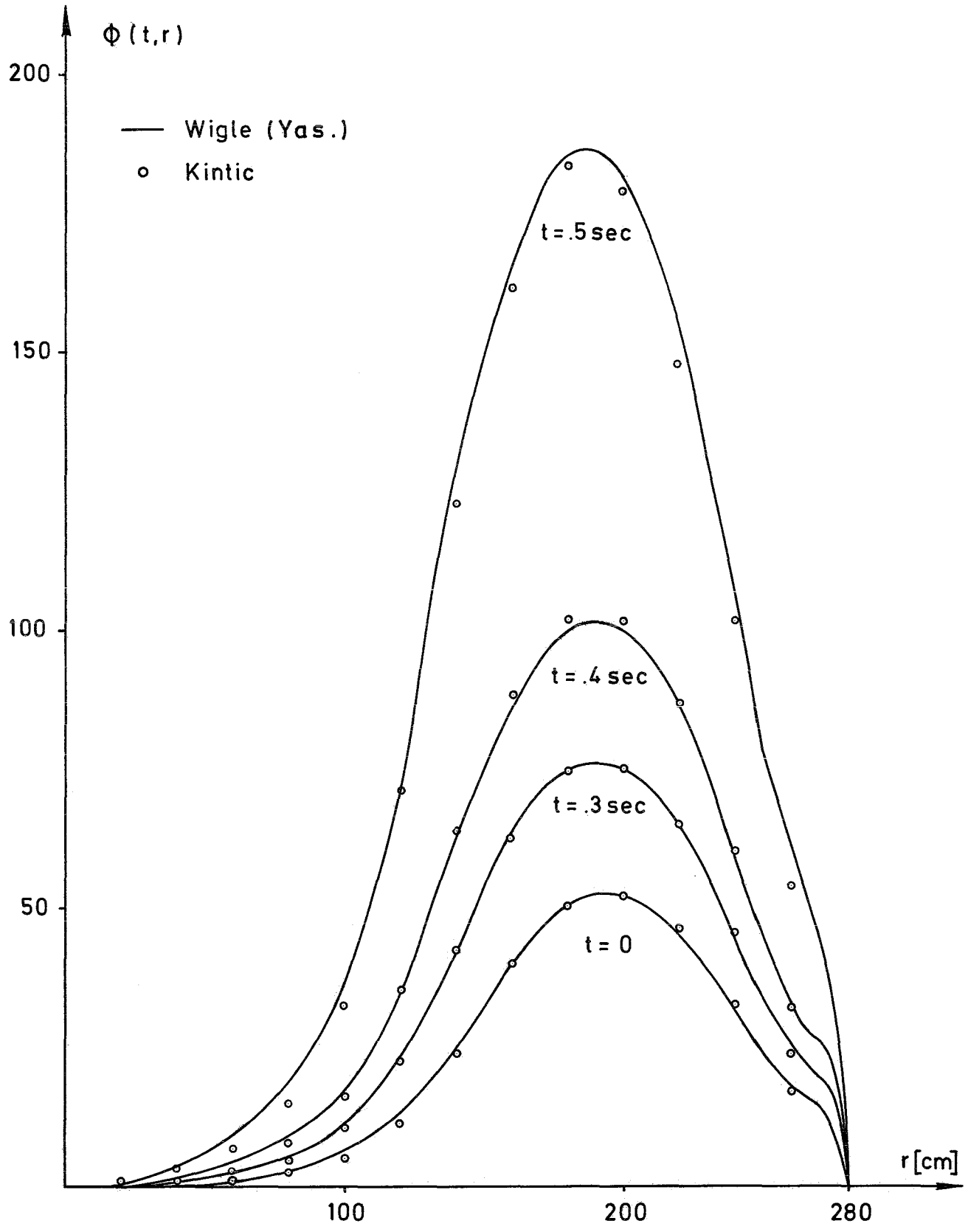

Fig. 8 : Axial flux distribution in the inner blanket for thermal reactor test case.

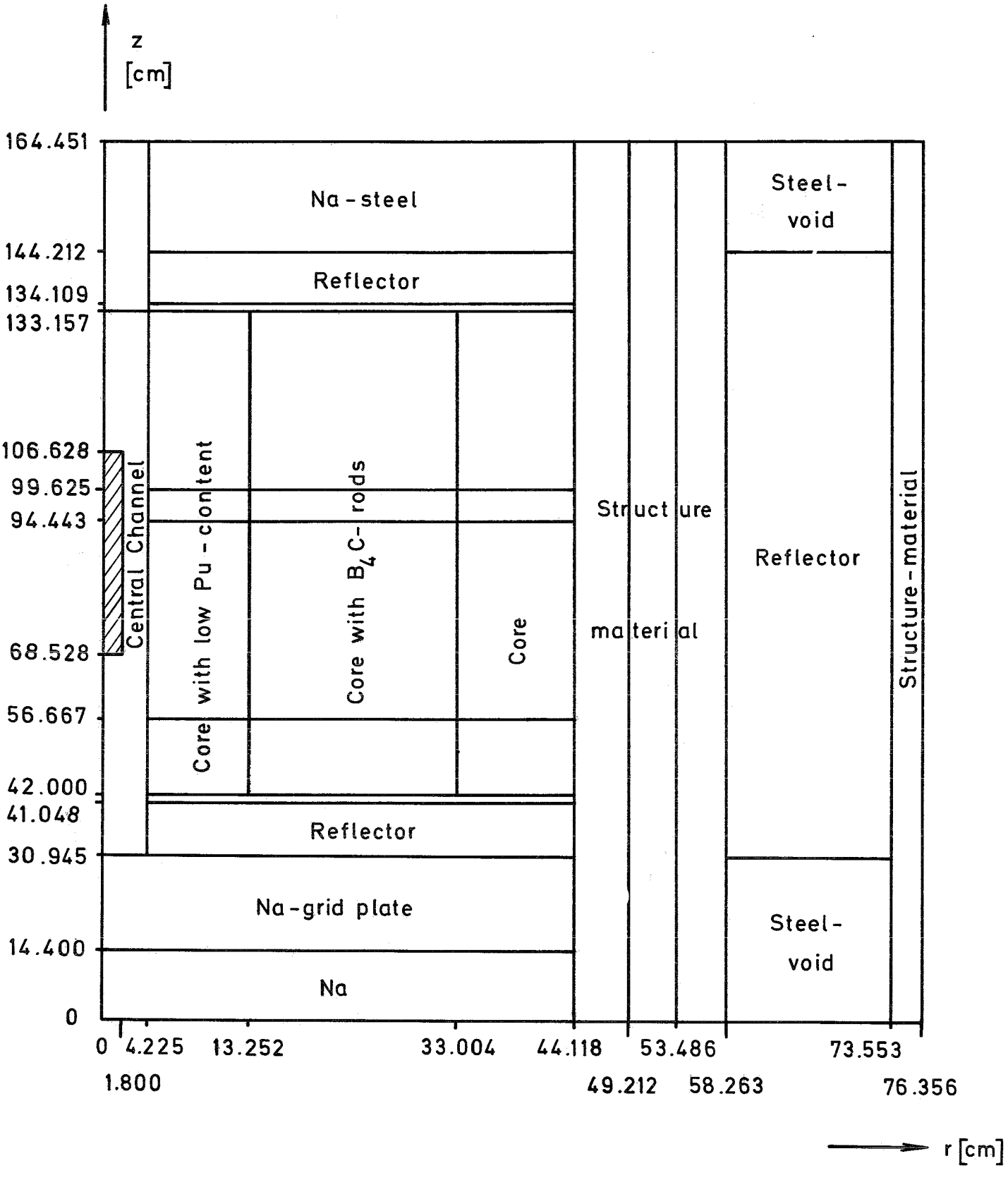

Fig. 9: Geometrical representation of SEFOR 1-D core.
The small zones between core and axial reflectors represent depleted UO_2 insulator pellets. Cross-hatched region: Initial position of absorber.

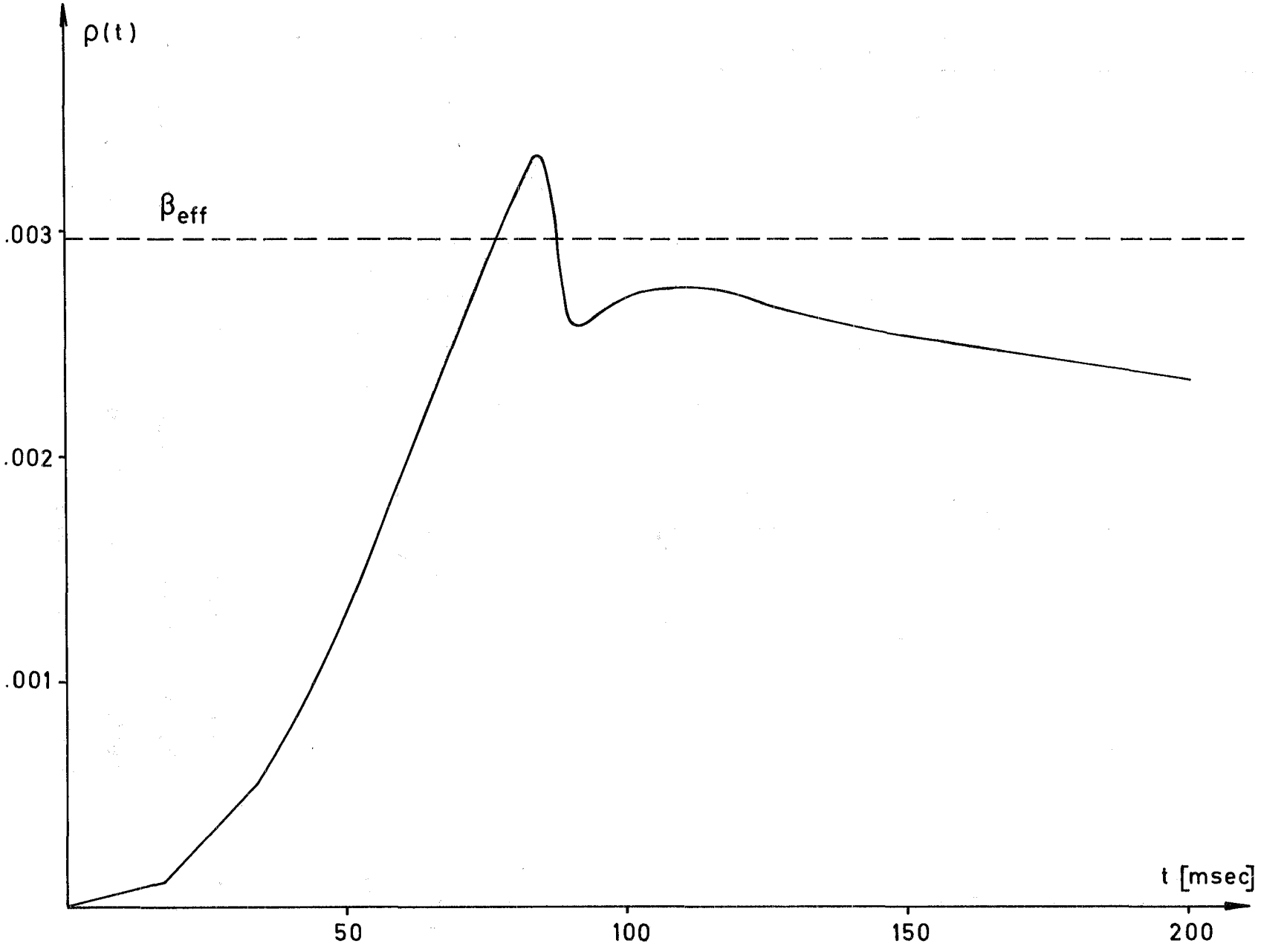

Fig. 10

Time dependence of reactivity for quasi-static approximation.

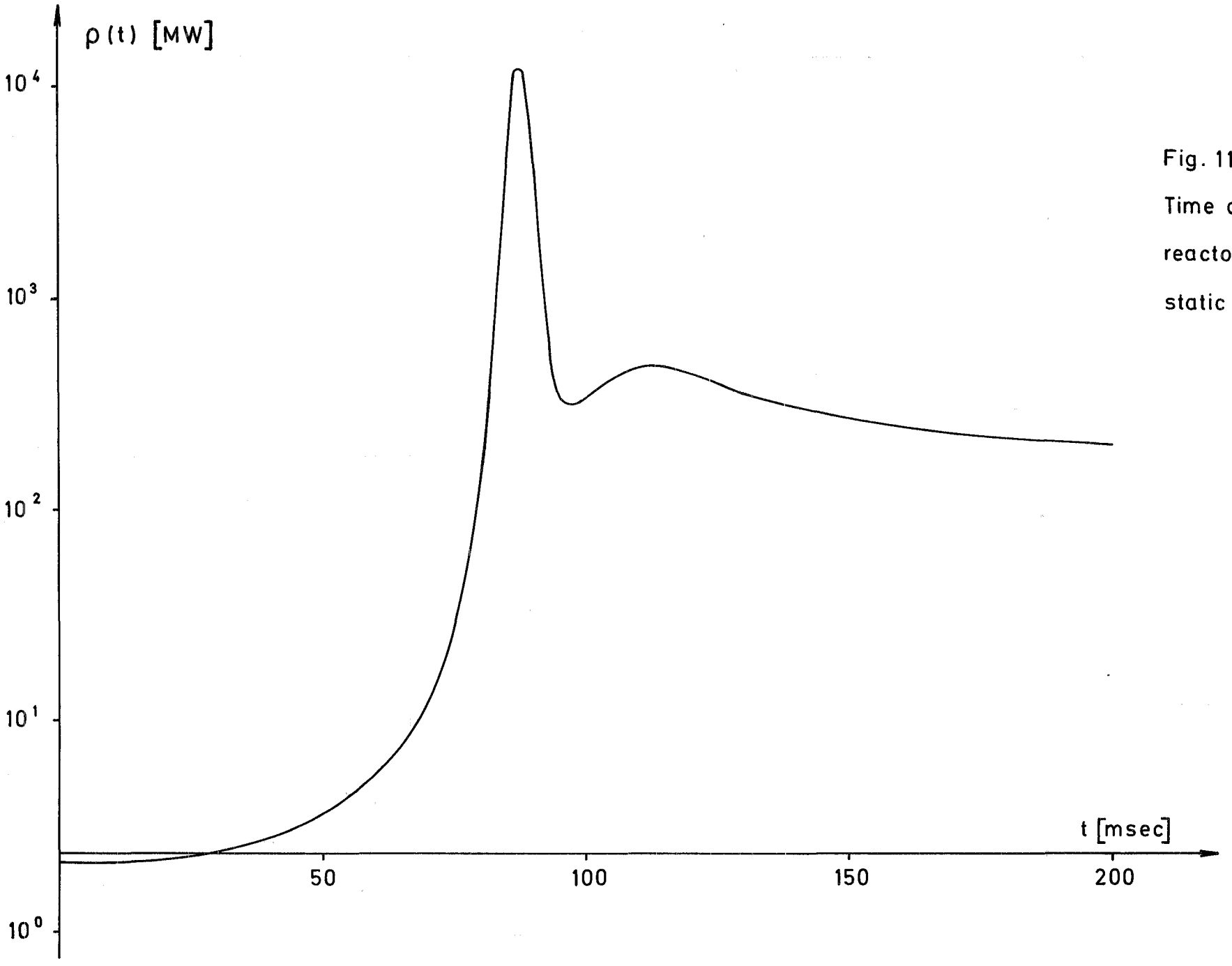

Fig. 11

Time dependence of reactor power for quasi-static approximation.

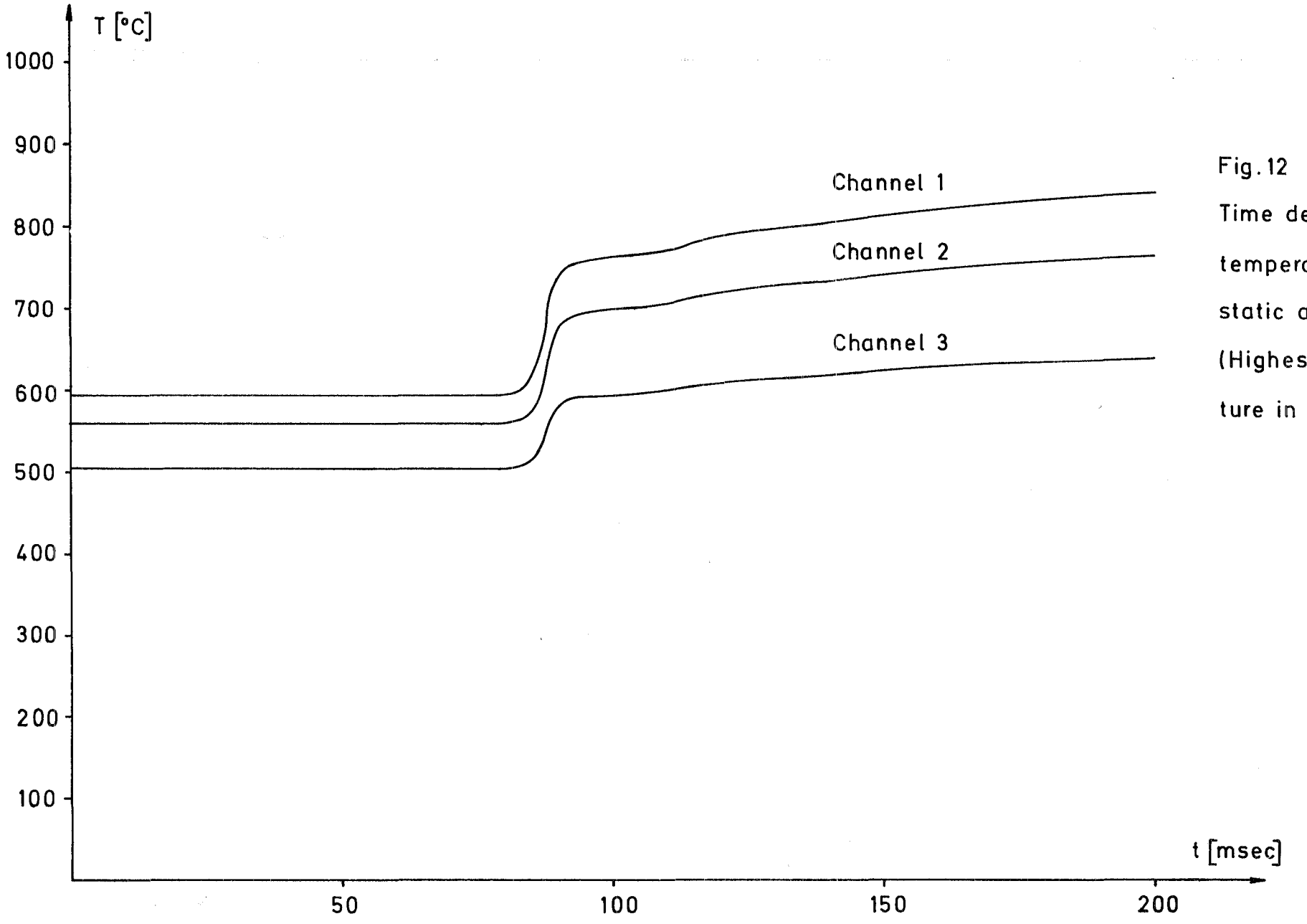

Fig. 12
Time dependence of temperatures for quasi-static approximation. (Highest central temperature in each channel)

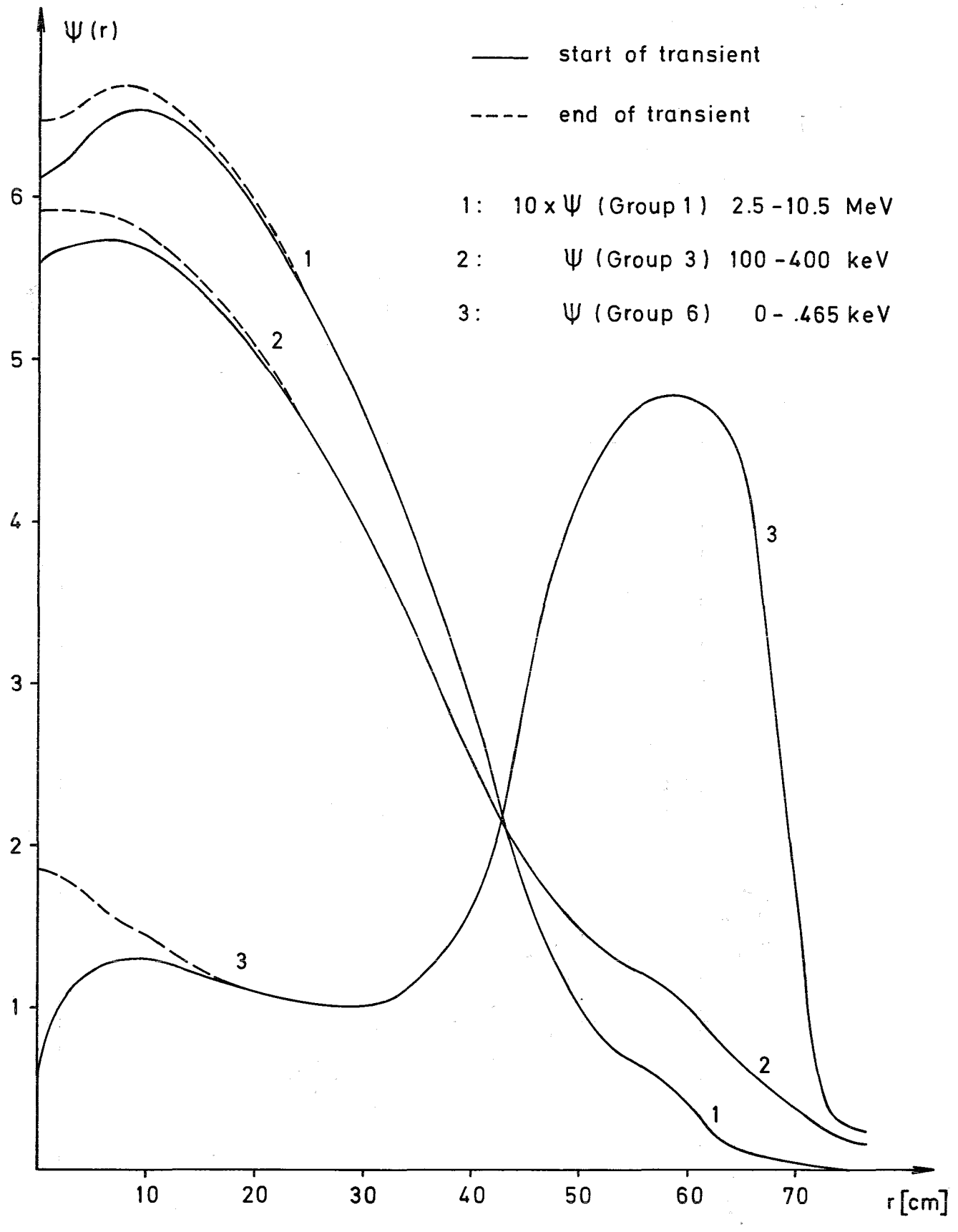

Fig. 13 : Radial group fluxes at start and end of SEFOR prompt critical transient; z = 94.443 cm

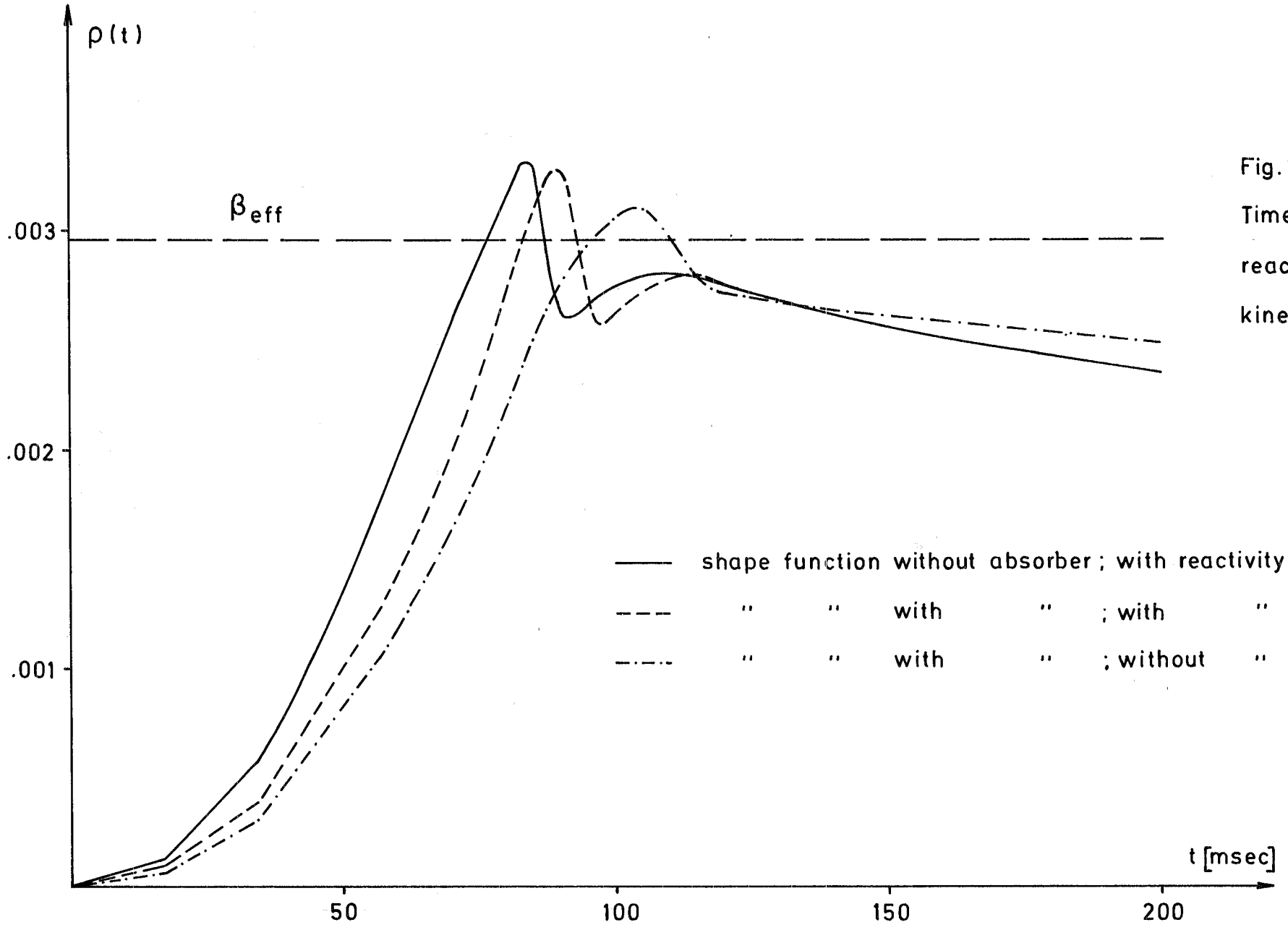

Fig. 14

Time dependence of reactivity for point kinetics calculations.

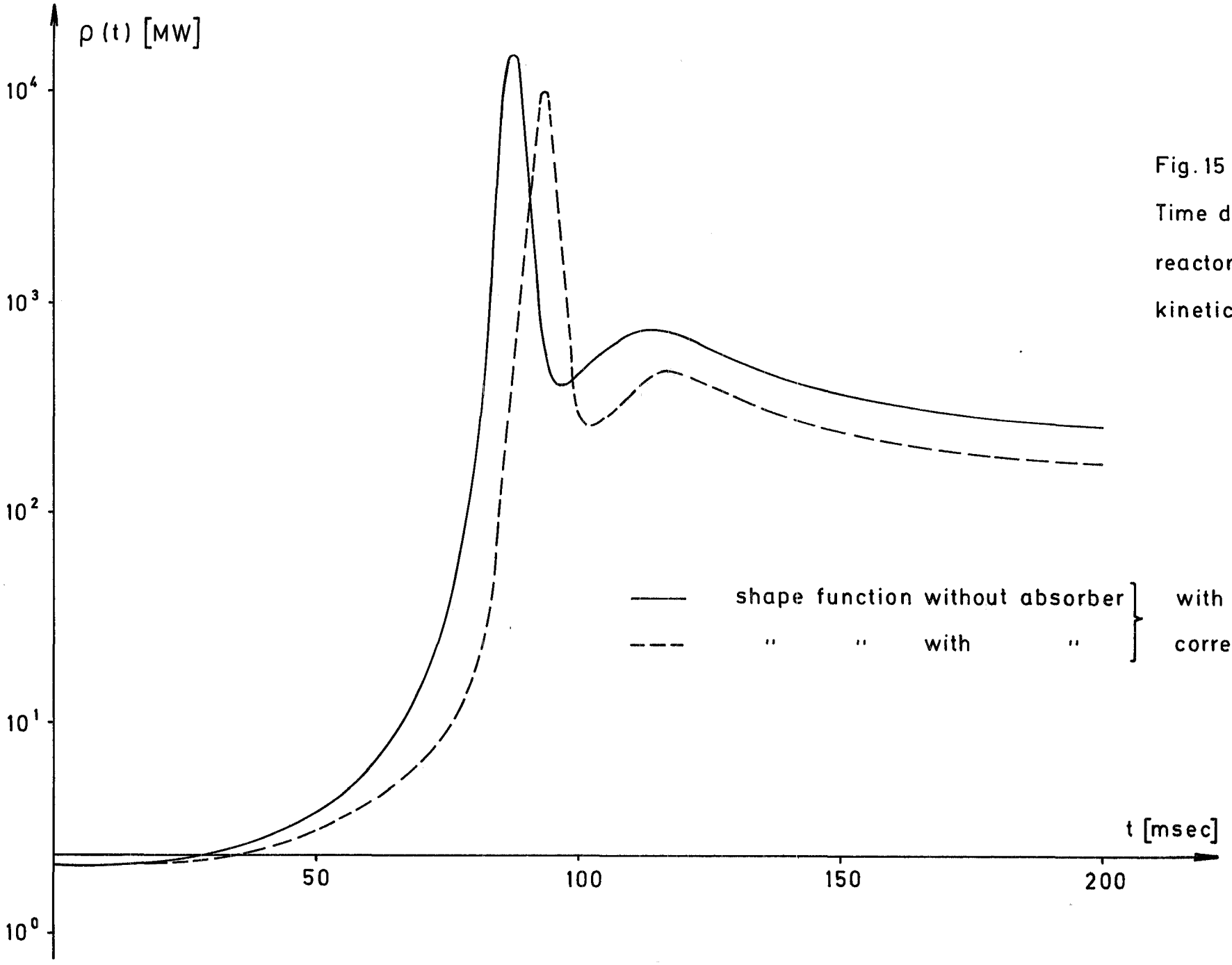

Fig. 15

Time dependence of reactor power for point kinetics calculations.

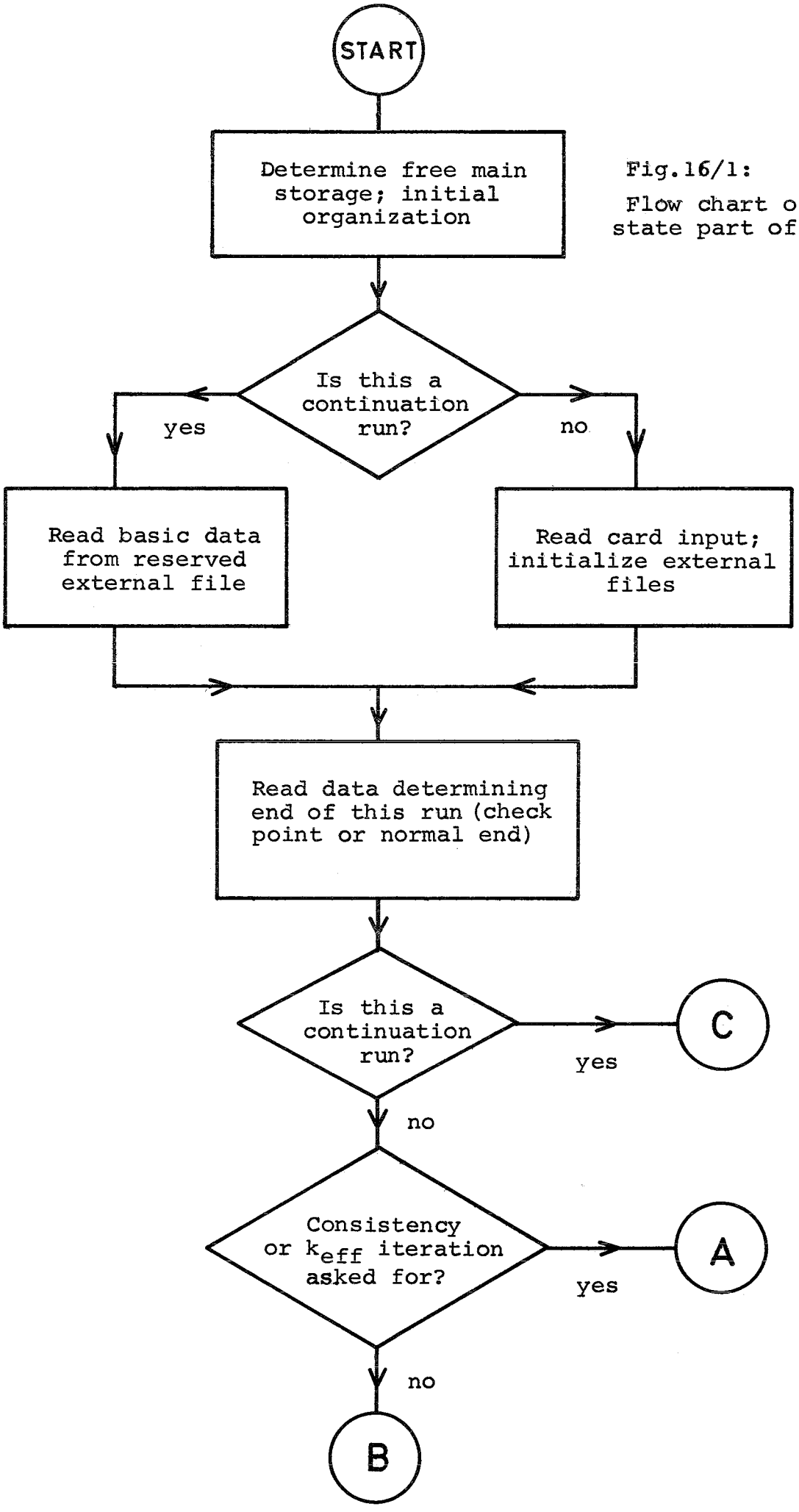

Fig.16/1:
Flow chart of steady state part of KINTIC-1

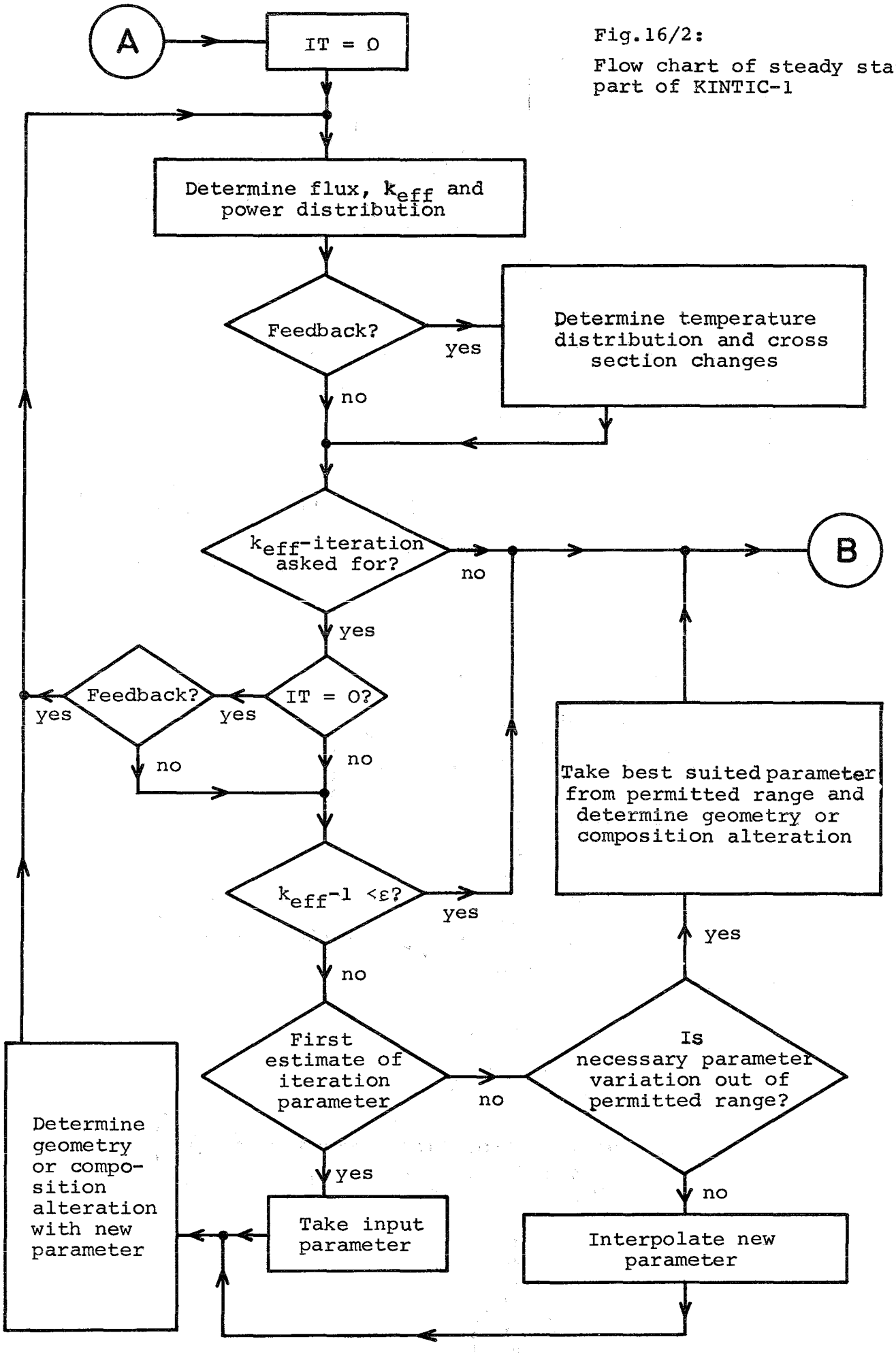

Fig.16/2:
Flow chart of steady state part of KINTIC-1

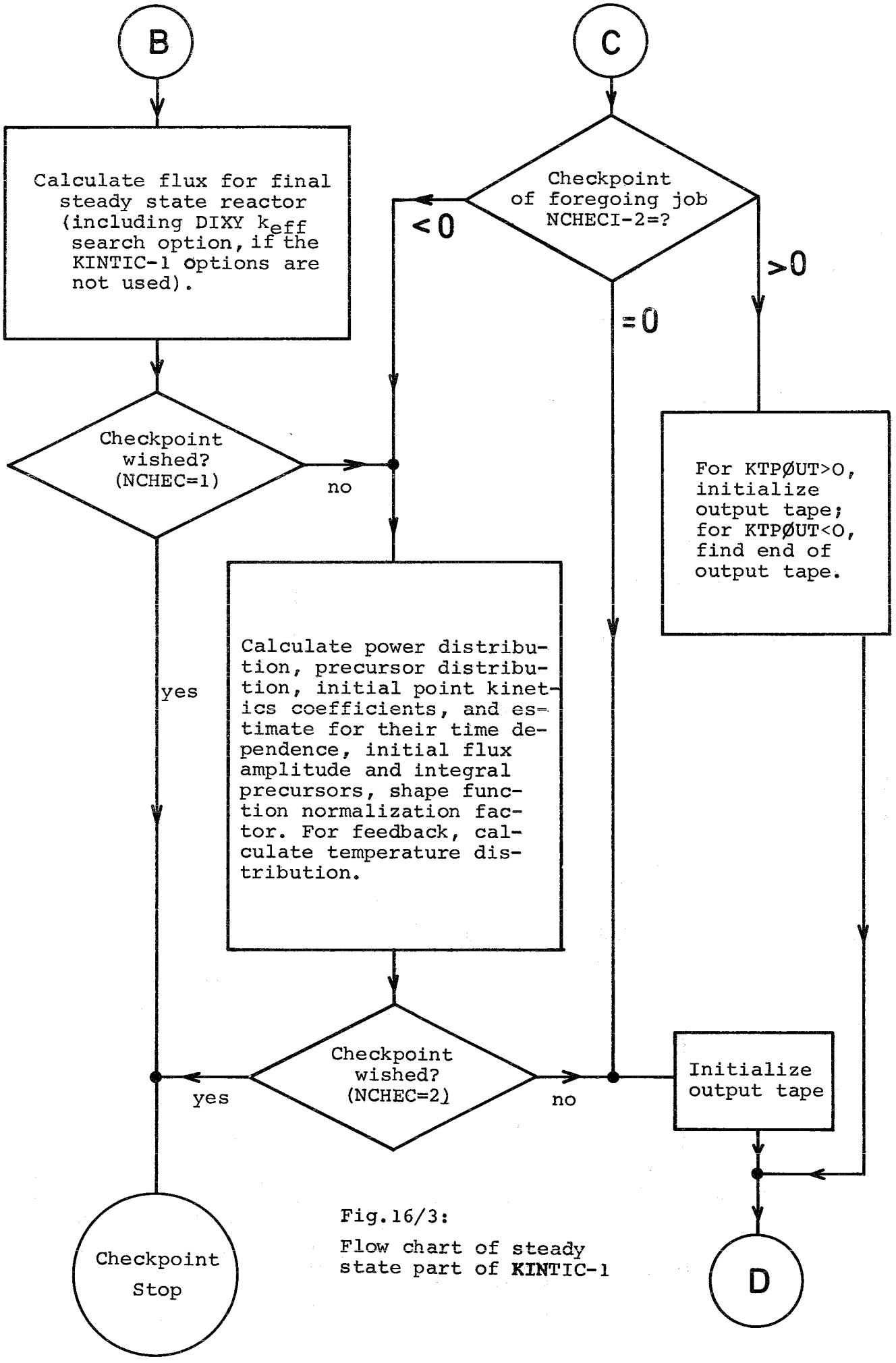

Fig.16/3:
Flow chart of steady state part of KINTIC-1

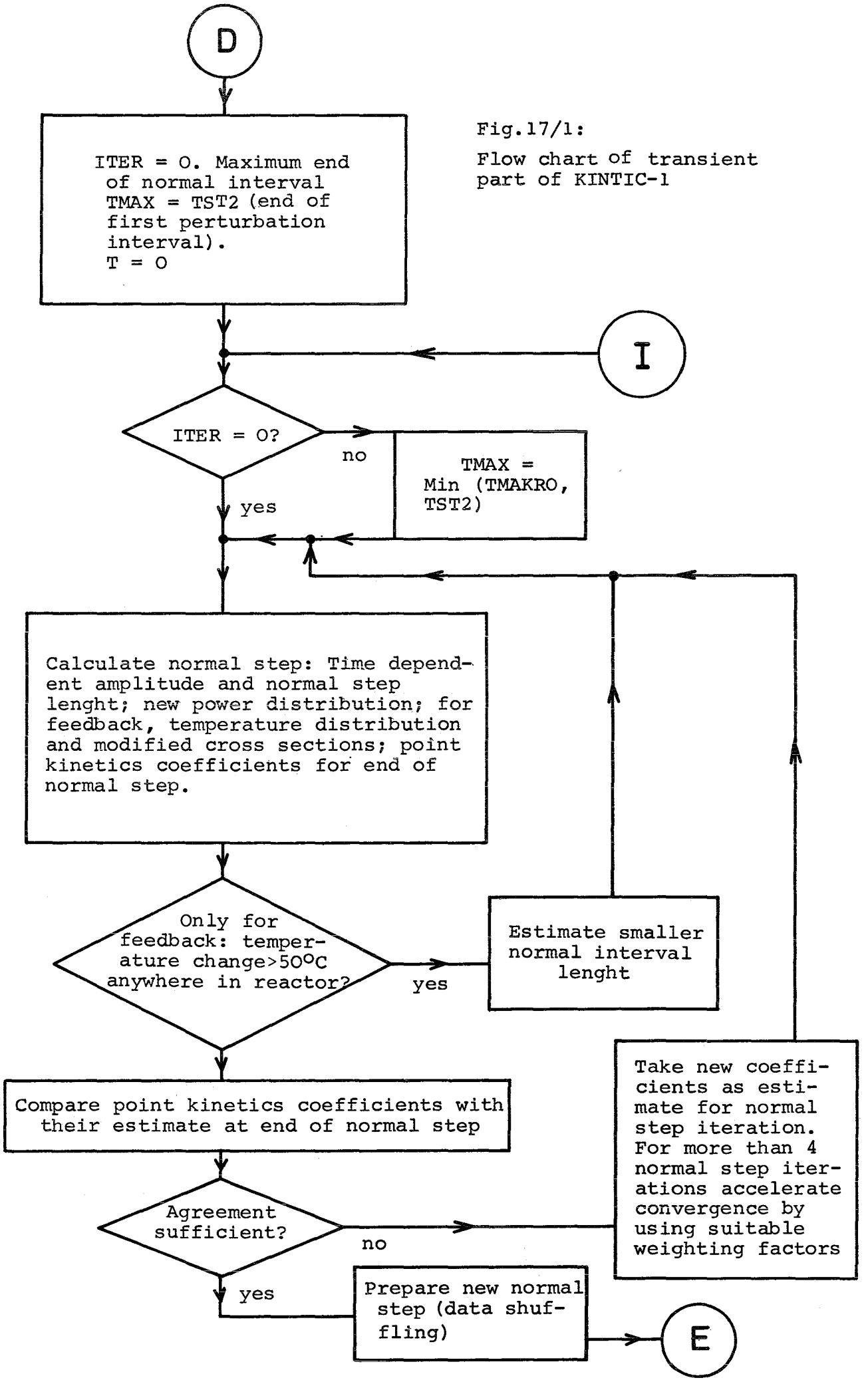

Fig.17/1:
Flow chart of transient part of KINTIC-1

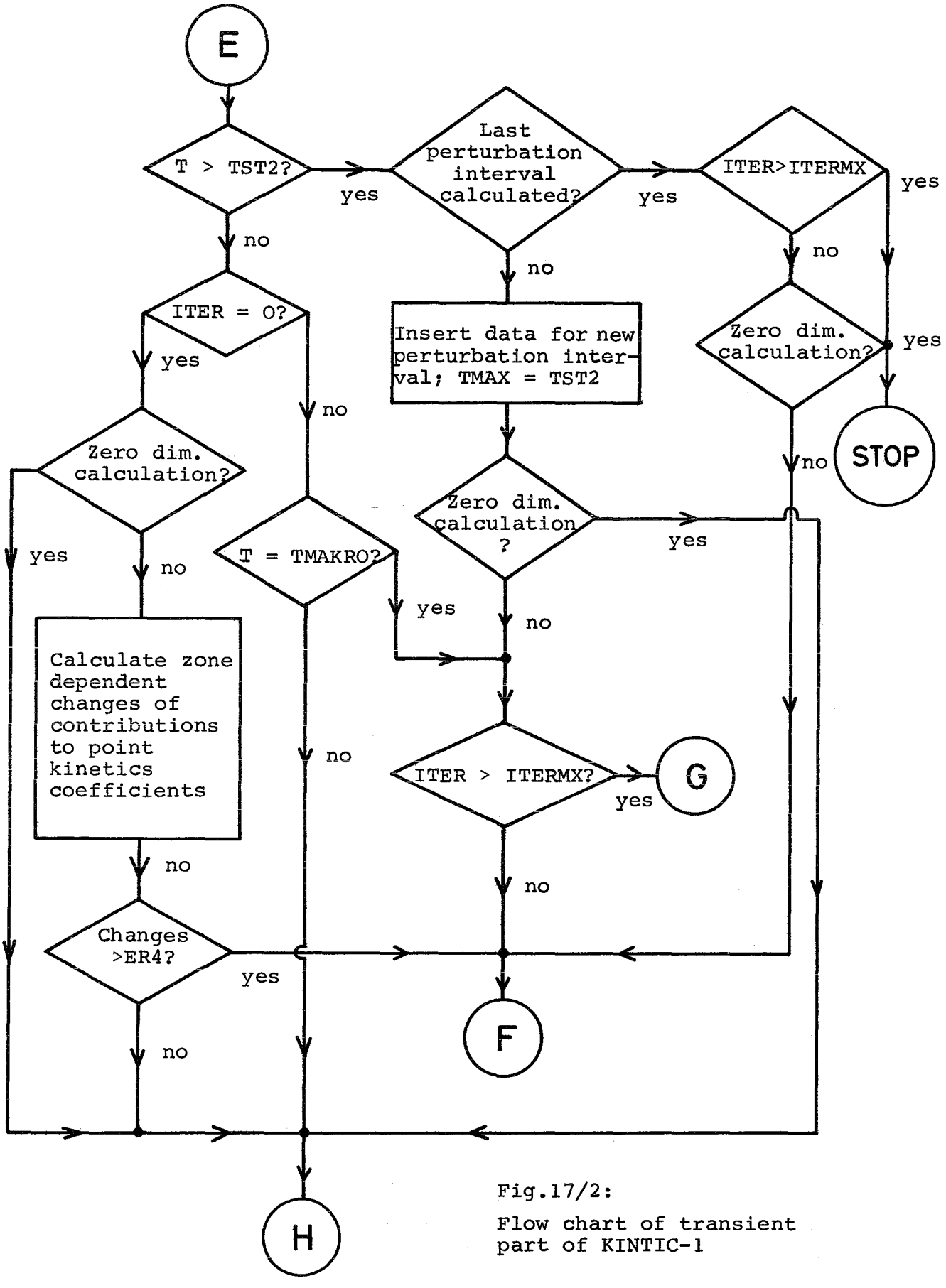

Fig.17/2:

Flow chart of transient part of KINTIC-1

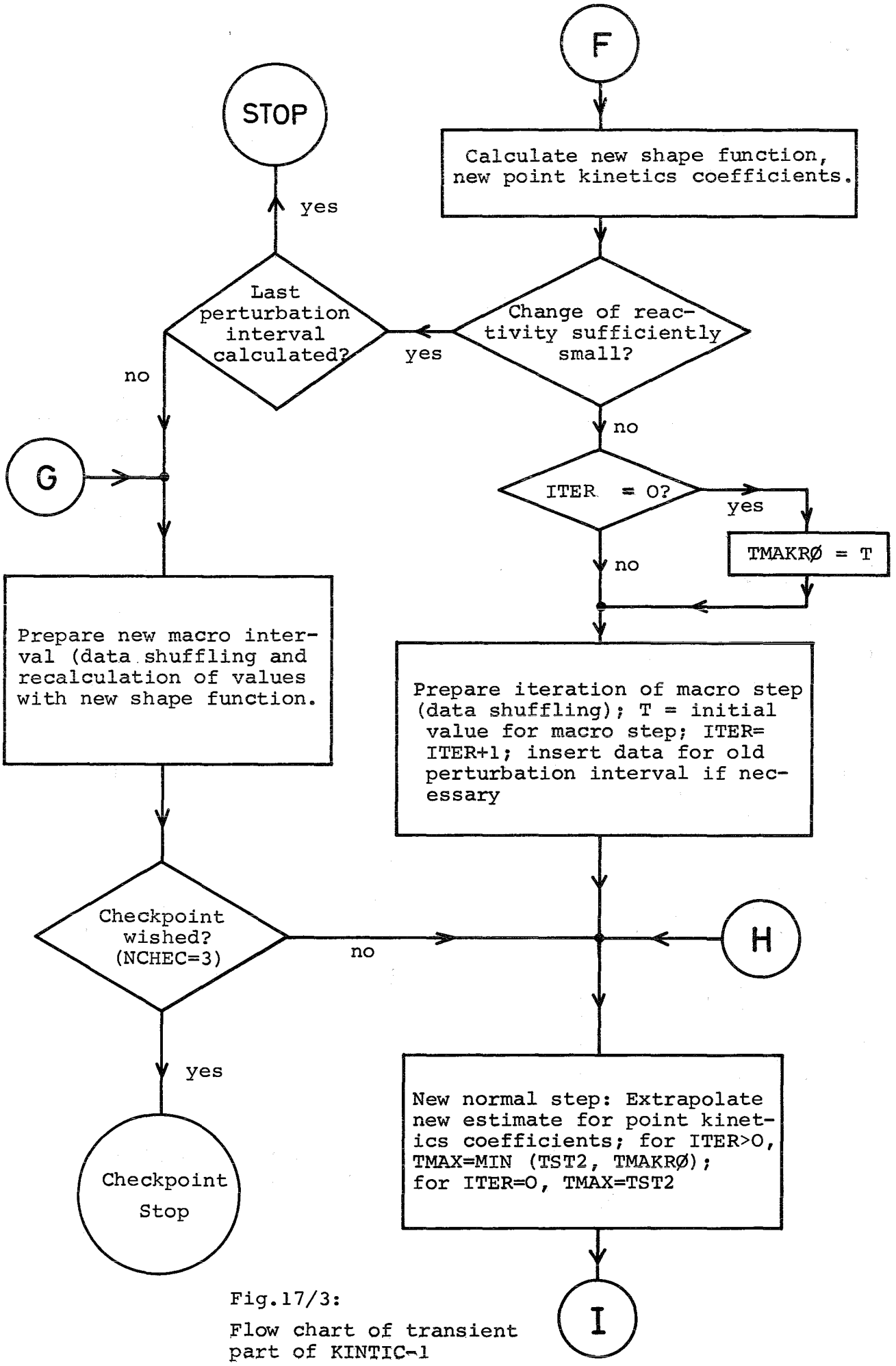

Fig.17/3:

Flow chart of transient part of KINTIC-1